

Instant cost and delayed reward. Demographic eco-evolutionary game dynamics under the impact of the delay resulting from the offspring maturation time.

Krzysztof Argasinski*,

Faculty of Mathematics Informatics and Mechanics

University of Warsaw

ul. Stefana Banacha 2

02-097 Warszawa

Poland

Ryszard Rudnicki

Institute of Mathematics of Polish Academy of Sciences

ul. Śniadeckich 8

00-656 Warszawa

Robert Szczelina

Faculty Of Mathematics and Computer Science

Jagiellonian University, ul. Łojasiewicza 6, 30-348 Kraków, Poland

Poland

*corresponding author: *argas1@wp.pl*

Acknowledgments: We would like to thank Mark Broom for support of the project. This paper was supported by the Polish National Science Centre Grant No.OPUS 2020/39/B/NZ8/03485 (KA) and in part by Polish National Science Centre Grant 2023/49/B/ST6/02801, and in part by NAWA Bekker Scholarship Program under grant no. BPN/BEK/2023/1/00170 (RS). **THIS IS A WORK IN PROGRESS VERSION, IN THE CASE OF DISCOVERED ERRORS PLEASE CONTACT THE CORRESPONDING AUTHOR**

Abstract

In this paper, we extend the demographic eco-evolutionary game approach, based on explicit birth and death dynamics instead of abstract "fitness" interpreted as an abstract "Malthusian parameter", by the introduction of the delay resulting from the juvenile maturation time. This leads to the application of the Delay Differential Equations (DDE). We show that delay seriously affects the resulting dynamics and may lead to the loss of stability of equilibria when critical delay is exceeded. We provide theoretical tools for the assessment of the critical delays and the parameter values when this may happen. Our results emphasize the importance of the mechanisms of density dependence. We analyze the impact of three different suppression modes based on: adult mortality, juvenile recruitment survival after the maturation period (without delay), and juvenile recruitment at birth (with the delay). The last mode leads to extreme patterns such as bifurcations, complex cycles, and chaotic dynamics. However, surprisingly, this mode leads to extension of the duration of the temporary transient metastable states known as "ghost attractors". In addition, we also focus on the problem of resilience of the analyzed systems against external periodic perturbations and feedback-driven factors such as additional predator pressure.

1 Introduction

George Evelyn Hutchinson's seminal essay, "The Ecological Theater and the Evolutionary Play" [1], underscored the vital connection between ecology and evolutionary theory. Presently, evolutionary biology research prioritizes eco-evolutionary synthesis, with a particular focus on understanding eco-evolutionary feedbacks [2, 3, 4, 5, 6, 7]. An example of such feedback within evolutionary game theory, was revealed by studies on demographic games [9, 10, 11]. This approach explored the interplay between ecological factors shaping the population dynamics and selection dynamics.

In contrast to standard evolutionary game theory [12, 13, 14, 15, 80, 16, 17], which links "payoffs" to "Darwinian fitness", the demographic approach considers two payoff functions related to reproductive success and the risk of death to the player. The definition of Darwinian fitness through demography and explicit balance between birth and death rates was advocated by [18, 19, 20, 21] and it solves the methodological issue known as "tautology problem" in evolutionary theory (the "fittest" survive and successfully reproduce, while the fittest are those with best survival and reproductive output, [22, 23, 24, 25]). The new approach emphasizes the importance of the density dependent growth limiting factors. In the standard replicator dynamics, the growth suppression can act through adult mortality, and cancels out in the replicator equation. In contrast, the approach of Argasinski and Broom assumes that the density dependence is driven by juvenile recruitment survival, described by logistic term acting on the fertility rate.

Recognizing the importance of density-dependent juvenile recruitment, further research explored more realistic suppression models than the classical logistic approach [26, 27, 28]. The demographic approach allowed for the development of replicator dynamics models, with explicit age structure [29] and state based replicator dynamics [28] related to the approach of Houston and McNamara [30]. This paved the way towards integrating the evolutionary game theory (focused on the evolution of behaviour) and life history theory (focused on the evolution of individual life cycles, [31, 32]). Due to clear mechanistic interpretation of parameters the demographic framework can be easily completed by individual based [33] or Monte Carlo simulations [34] acting as *in silico* experiments.

In this paper we will investigate the impact of the important life history parameter, which is maturation time, on the population dynamics and the trajectories of selection. Because models with explicit age structure [29] are complicated, in our initial research we will use much simpler but still interesting approach based on delay differential equations. Delay differential equations are already used in evolutionary game theory ([35, 36, 37, 38, 39, 40] and the references therein). However, combination of delays and demographic approach can be very profitable. When we add delay to fertility payoff functions it can be interpreted as the maturation or egg hatching time, very important parameter from the biological point of view. This will introduce aspect related to life history theory [31, 32] into game theoretic framework, which was advocated by [41]. However, the resulting impact will be much broader and important from the point of view of the questions on the definition of Darwinian fitness and its role in modelling and theoretical framework.

List of important symbols:

n_i	number of i -strategy individuals
e_i	i -th canonical unit vector
$n = n_1 + n_2$	populations size
$q_i = n_i/(n_1 + n_2)$	frequency of the i -th strategy
$\tau = 1$	virtual interaction rate allowing for demographic interpretation of payoffs in differential equation
V	fertility matrix, entries $V_{i,j}$ describe number of offspring produced during game round between i and j strategy carriers
D	mortality payoff matrix, entries $D_{i,j}$ describe probability of death of i th strategy player during the game round against j th strategy opponent
Φ	background fertility rate (intensity of the background birth)
Ψ	background mortality rate (intensity of the background death)
$\left(1 - \frac{n(t)}{K}\right)$	logistic juvenile recruitment survival, proportional to the fraction of free nest sites
K	carrying capacity interpreted as the number of nest sites
$\Omega n(t)$	phenomenological linear density dependent mortality
$u^{n(t-\tau)/z}$	phenomenological juvenile survival with delay in argument $u \in \langle 0, 1 \rangle$ and z is the scale parameter describing the population size where juvenile survival equals u

2 Methods and technical details from previous papers:

The general model from previous papers [9, 10, 11] is as follows:

Assume two competing strategies and we have n_i individuals of each strategy.

To be used in differential equations, demographic payoff functions V (describing the number of offspring resulting from a game round) and D (probability of death during a game round) should be multiplied by virtual interaction rate τ describing the intensity of the occurrence of the focal game rounds. Background mortality and fertility rates are adjusted to the timescale where $\tau = 1$. In effect, this parameter can be not explicitly present in the equations, while producing the correct unit of the.

Starting point is the system of the Malthusian growth equations:

$$\frac{dn_i}{dt} = n_i(t) [(\tau e_i V q^T(t) + \Phi) \mathbf{D}(n(t)) - \tau e_i D q^T(t) - \Psi] \text{ for } i = 1, 2 \quad (1)$$

where:

e_i i -th canonical unit vector

$n = n_1 + n_2$ populations size

$q_i = n_i/n$ i -th strategy frequency

$\tau = 1$ virtual interaction rate allowing for demographic interpretation of payoffs in differential equation, which is described below

V fertility matrix, entries $V_{i,j}$ describe number of offspring produced during game round

D mortality payoff matrix, entries $D_{i,j}$ describe probability of death of i th strategy player during the game round against j th strategy opponent

Φ background fertility rate (intensity of the background birth)

Ψ background mortality rate (intensity of the background death)

$\mathbf{D}(n(t))$ -juvenile recruitment survival. Previous works used the logistic term $\left(1 - \frac{n(t)}{K}\right)$, proportional to the fraction of free nest sites. Thus every newborn checks single random nest site. If it is free then it survives if it is occupied, it dies. Generalizations are possible.

K carrying capacity interpreted as the number of nest sites [42]

Then we can rescale equations (1) to replicator dynamics by change of coordinates where $q = [q_1, 1 - q_1]$ is the vector of strategy frequencies where $q_1 = n_1/(n_1 + n_2)$ and $n = n_1 + n_2$ is population size

$$\frac{dq_1}{dt} = q_1(t) \left[(e_1 V q^T(t) - q(t) V q^T(t)) \mathbf{D}(n(t)) - (e_1 D q^T(t) - q(t) D q(t)) \right] \quad (2)$$

$$\frac{dn}{dt} = n(t) \left[q(t) V q^T(t) \mathbf{D}(n(t)) - q(t) D q(t) + \Phi \mathbf{D}(n(t)) - \Psi \right] \quad (3)$$

Zeros of the bracketed terms from equations (2) and (3) will constitute frequency and density nullclines: $\tilde{q}(n)$ and $\tilde{n}(q)$. Intersections of those surfaces will constitute stable and unstable rest points.

2.1 Resilience against seasonal perturbations and external feedback driven by predator pressure

We can analyze our model from the point of view of the resilience of the system (sensu Holling), defined as the propensity to absorb the perturbation altering the state while maintaining the functions of the system [43, 44, 77, 45, 46, 47]. Thus the question is how the system will react to the external perturbation caused by external environmental factors or additional feedbacks. In the so-called "flow-kick" approach [45], perturbation is represented by a discrete shift of the population state followed by a continuous return phase, modeled by a standard autonomous differential equation. This approach is termed impulse differential equation [48]. In contrast to that, we will incorporate the perturbation as the explicit part of the model, expressed as external mortality pressures (such as periodic mortality or explicit predator pressure), similarly to the Lotka-Volterra models with forcing [49, 50, 51, 52, 53, 54]. This approach to the resilience analysis is conceptually related to the structural stability [55, 56], but within the biological context of the model, since perturbation should have biological interpretation. It is also linked to the concept of permanence ([57, 58, 59, 60, 61, 62]). It is defined as the existence of the attracting region in the interior of the phase space bounded from extinction. Then the system can resist frequent small perturbations and rare big events. Therefore, this system can be completed by addition of terms describing the impact of strategically neutral (i.e. acting on all strategies in the same way) external environmental factors, such as seasonality or predator pressure. Seasonality may act as a periodic mortality factor $\alpha(1 + \sin(\theta t))$ added to the population size equation (3), where α describes mortality amplitude and θ is the duration of the season. Impact of the predator population feedback (denoted by variable $p(t)$) can act on the equation (3) via another per capita mortality factor $p_x(t)$ and the additional equation for the dynamics of the predator population size

$$\frac{dx}{dt} = x(t) b_p n(t) - x(t) d_p. \quad (4)$$

2.2 Hawk-Dove example without delays

Classical Hawk-Dove game can be used as the illustrative example. In the classical case when population grows exponentially or the growth is suppressed by some selectively neutral adult mortality, matrix $V - d$ is the classic Hawk-Dove matrix

$$U = \left(\begin{array}{c|cc} & H & D \\ \hline H & 0.5(F-d) & F \\ D & 0 & 0.5F \end{array} \right).$$

According to the demographic interpretation in every Hawk vs. Hawk contest winner consumes fertility reward F while loser can die with probability d . Thus payoff matrix $U = V - D$ can be decomposed into separate fertility and mortality payoff matrices:

$$V = \left(\begin{array}{c|cc} & H & D \\ \hline H & 0.5F & F \\ D & 0 & 0.5F \end{array} \right) \quad \text{and} \quad D = \left(\begin{array}{c|cc} & H & D \\ \hline H & 0.5d & 0 \\ D & 0 & 0 \end{array} \right)$$

Then the demographic payoffs are:

$$V_h = [(1 - q_d)0.5 + q_d] F = 0.5(1 + q_d) F \quad \text{Hawk fertility payoff} \quad (5)$$

$$V_d = q_d 0.5F + (1 - q_d)0 = q_d 0.5F \quad \text{Dove fertility payoff} \quad (6)$$

$$\bar{V} = (1 - q_d)V_h + q_d V_d = 0.5F \quad \text{average fertility payoff} \quad (7)$$

and

$$D_h = (1 - q_d)0.5d \quad \text{Hawk mortality payoff} \quad (8)$$

$$D_d = 0 \quad \text{Dove mortality payoff} \quad (9)$$

$$\bar{D} = (1 - q_d)^2 0.5d \quad \text{average mortality payoff} \quad (10)$$

After substitution of the above payoff functions to equations (2,3)

$$\frac{dq_d}{dt} = 0.5q_d(t)(1 - q_d(t))((1 - q_d(t))d - \mathbf{D}(n(t))F) \quad (11)$$

$$\frac{dn}{dt} = n(t) \left((0.5F + \Phi) \mathbf{D}(n(t)) - \left[(1 - q_d(t))^2 0.5d + \Psi \right] \right). \quad (12)$$

Flat trivial nullclines for the values $q_d = 0$, $q_d = 1$ and $n = 0$ describe the boundaries of the phase space and extinction of respectively Doves, Hawks and the whole population. Nontrivial frequency and density nullclines for this system are following

$$\tilde{q}_d(n) = 1 - \mathbf{D}(n(t)) \frac{F}{d} \quad (13)$$

$$\mathbf{D}(n(t)) = \frac{(1 - q_d(t))^2 0.5d + \Psi}{0.5F + \Phi} \quad (14)$$

and for any monototnusly decreasing, density dependent juvenile recruitment survival $\mathbf{D}(n(t))$ the density nullcline is

$$\tilde{n}(q) = \mathbf{D}^{-1} \left(\frac{(1 - q_d(t))^2 0.5d + \Psi}{0.5F + \Phi} \right),$$

and both nullclines intersect when

$$\Delta = \left(\frac{\Phi}{F} + 0.5 \right)^2 - 2 \frac{\Psi}{d} > 0,$$

and we have two intersections

$$\begin{aligned} \check{q}_d &= 0.5 - \frac{\Phi}{F} - \sqrt{\Delta} = 0.5 - \frac{\Phi}{F} - \sqrt{\left(\frac{\Phi}{F} \right)^2 + \frac{\Phi}{F} - 2 \frac{\Psi}{d} + 0.25} \\ \hat{q}_d &= 0.5 - \frac{\Phi}{F} + \sqrt{\Delta} = 0.5 - \frac{\Phi}{F} + \sqrt{\left(\frac{\Phi}{F} \right)^2 + \frac{\Phi}{F} - 2 \frac{\Psi}{d} + 0.25}, \end{aligned}$$

and above frequencies of intersections do not depend on the form of the juvenile survival $\mathbf{D}(n(t))$. Then the respective population sizes are:

$$\begin{aligned} \check{n} &= \mathbf{D}^{-1} \left(\frac{d}{f} \left(0.5 + \frac{\Phi}{f} \right) - \sqrt{\Delta} \right) = \mathbf{D}^{-1} \left(\frac{d}{f} \left(0.5 + \frac{\Phi}{f} \right) - \sqrt{\left(\frac{\Phi}{F} \right)^2 + \frac{\Phi}{F} - 2 \frac{\Psi}{d} + 0.25} \right) \\ \hat{n} &= \mathbf{D}^{-1} \left(\frac{d}{f} \left(0.5 + \frac{\Phi}{f} \right) + \sqrt{\Delta} \right) = \mathbf{D}^{-1} \left(\frac{d}{f} \left(0.5 + \frac{\Phi}{f} \right) + \sqrt{\left(\frac{\Phi}{F} \right)^2 + \frac{\Phi}{F} - 2 \frac{\Psi}{d} + 0.25} \right) \end{aligned}$$

For the logistic suppression $\mathbf{D}(n(t)) = \left(1 - \frac{n(t)}{K} \right)$, the density nullcline (also termed stationary density surface [78]) is:

$$\tilde{n}(q) = \left[1 - \frac{(1 - q_d)^2 0.5d + \Psi}{0.5F + \Phi} \right] K,$$

and the population sizes at the rest points will be

$$\begin{aligned}\check{n} &= \left[1 - \frac{d}{f} \left(0.5 + \frac{\Phi}{f} \right) + \sqrt{\Delta} \right] K \\ \hat{n} &= \left[1 - \frac{d}{f} \left(0.5 + \frac{\Phi}{f} \right) - \sqrt{\Delta} \right] K\end{aligned}$$

Detailed derivation is in the Appendix 1.

Those intersections constitute the rest points of the system if they are contained in the phase space $[0, 1] \times [0, K]$. When Δ has a small negative value then both nullclines disconnect and form a narrow channel attracting trajectories and trapping them for a longer time. Then the system pretends to be in the stable state and afterwards it rapidly switches to the real stable attractor. Narrow channel trapping the trajectories is called a ghost attractor and the resulting pattern in time is termed a long transient behaviour [64, 65, 66]. As we mentioned before. Equation (12) can be completed by additional mortality factors describing seasonality, or predator impact (then the system (11,12) can be completed by equation (4) describing the predator population). Similarly, the seasonality can be described by periodic background mortality, which will indirectly affect the frequency dynamics. Both factors will be presented in detail in the Results section.

3 Results

3.1 Abstract "fitness" or explicit births and deaths? Interaction rates, pair formation and the timing of interaction events

Traditionally payoff functions are interpreted as differences in the resulting growth rates $U_i = V_i - D_i$, without explicit distinction between fertility and mortality rates. This leads to the conceptual limitations of the classical framework. Darwinian fitness (thus a game payoff) is defined as the long term growth rate, while in replicator equation, growth rate is defined as proportional to the payoff. To summarize, since fitness is defined as the growth rate, then, in this model, growth rate is defined as "growth rate". This is related to the widely discussed the so-called tautology problem in evolutionary theory [22, 23, 24, 25] (the survival and reproduction of the fittest are those with the greatest survival and reproduction). Rates of increase $n_i U_i$, are expressed as numbers of individuals per unit time. Therefore, a unit of payoff U_i (i.e., the per capita fitness) should be $1/(\text{time unit})$. Since for small Δt the population increases as $n_i(t + \Delta t) - n_i(t) = n_i(t)U_i\Delta t$, the phenomenological dimensionless scaling factor $U_i\Delta t$ describes how many more individuals will be " Δt later". We cannot measure this value at time t , we can try to estimate it post factum at $t + \Delta t$. This value should be rather a prediction generated by a model with parameters measurable, at time t , i.e. "now". In such a framework we cannot build a fully predictive model based on some properties of the interacting agents. We must attribute to them some abstract growth rates, which we can try to estimate post factum since we cannot measure them at time t .

This leads to a fundamental question about the biological/physical meaning of the cost d and benefit f parameters in the payoff matrix. They turns out to be unspecified increments and decrements of some unspecified growth rate (thus cost describes unborn descendants). Such vague connection to biological realism, in particular, experimental measurements of parameters limit the quantitative description and the explanatory power of the models [41].

Therefore, decomposition of the constant abstract fitness into separate birth and death rates $U_i = \tau V_i - \tau D_i$ allows for mechanistic interpretation and increases the framework's predictive power. Note that the model still can be expressed in terms of differences in constant "fitnesses" U_i . However, when we add the maturation delay γ , birth rate becomes $n(t - \gamma)V_i$ while the death rate is still $n(t)D_i$. then the per capita growth rate has the form:

$$n_i(t)U_i = n(t) \left[\frac{n(t - \gamma)}{n(t)} V_i - D_i \right].$$

Therefore, this parameter has the different values when the population is growing or declining. Thus, in this case we cannot derive the constant and independent of time "fitness effect" resulting from the game interaction. This shows that the additive quantity called "fitness" simply do not exists in that case.

3.2 Meaning and interpretation of the time unit

For the interaction rate τ the per capita average time between game interaction equals $1/\tau$. By definition, interaction intensity is the derivative of per capita probability of playing the game round. However, this suggests that each individual can be described as the independent Poisson process. The problem is that for each game round we need two players. Therefore, the modelling framework should explicitly consider the dynamics of pair formation. From the perspective of the whole population, number of individuals that played at least single game round is described by equation $\dot{n}(t) = n(t)\tau$. For small time intervals Δt this equation can be approximated by first order Taylor expansion

$$n(t + \Delta t) = n(t) + \dot{n}(t)\Delta t \quad (15)$$

$$n(t + \Delta t) - n(t) = n(t)\tau\Delta t \quad (16)$$

Therefore τ is equal to the fraction of the population that participated in at least single game round during small Δt . Since for each game round we need two players, during Δt interval $\tau n(t)\Delta t/2$ game rounds will be played. For the timescale where interaction rate equals 1 average per capita time between interaction events also equals 1. This interpretation of the time unit will be important for the evaluation of the value of the delay resulting from maturation time. Hence the fraction of individuals that played at least a single game round during a short interval $\Delta t \ll 1$ equals to Δt . Then, the dynamics of the game rounds occurrence (with birth and deaths ignored) follows the exponential decay $n_i(t_0)e^{-t}$ (a solution of the equation $dn_i/dt = -\tau n_i$ with intensity $\tau = 1$). This implies that during single time unit, fraction $1 - e^{-1}$ of individuals present at the t_0 , have not played the focal game (however, they can die and reproduce due to the background events).

3.3 Methods used in analysis of the impact of the delays

In this section we will introduce the methods used for the analysis of the impact of delay on stability of the rest points.

3.3.1 Analytical toolbox

Let us introduce the method to calculate of the critical bifurcation delay as the function of the model parameters in general two dimensional systems described by variables x, y . First Let $x_\gamma(t) = x(t - \gamma)$, $y_\gamma(t) = y(t - \gamma)$. Consider the general system of the form

$$x' = f_1(x, x_\gamma, y, y_\gamma), \quad (17)$$

$$y' = f_2(x, x_\gamma, y, y_\gamma), \quad (18)$$

where f_1 and f_2 are continuously differentiable functions. Let (x^*, y^*) be a rest point of this system, i.e. x^* and y^* satisfy the conditions $f_1(x^*, x^*, y^*, y^*) = 0$ and $f_2(x^*, x^*, y^*, y^*) = 0$. Let

$$b_{11} = \frac{\partial f_1}{\partial x}, \quad b_{12} = \frac{\partial f_1}{\partial x_\gamma}, \quad b_{13} = \frac{\partial f_1}{\partial y}, \quad b_{14} = \frac{\partial f_1}{\partial y_\gamma},$$

$$b_{21} = \frac{\partial f_2}{\partial x}, \quad b_{22} = \frac{\partial f_2}{\partial x_\gamma}, \quad b_{23} = \frac{\partial f_2}{\partial y}, \quad b_{24} = \frac{\partial f_2}{\partial y_\gamma},$$

$$a_{11} = b_{11} + b_{12}, \quad a_{12} = b_{13} + b_{14},$$

$$a_{21} = b_{21} + b_{22}, \quad a_{22} = b_{23} + b_{24}.$$

In the formulas for the coefficients b_{ij} , we calculate the partial derivatives of the function f at the point (x^*, x^*, y^*, y^*) .

Theorem 1 *Let \mathbf{A} be the matrix of the form $\mathbf{A} = [a_{ij}]$, $1 \leq i, j \leq 2$. Assume that the rest point (x^*, y^*) of system (17)–(18) is locally stable for $\gamma = 0$. Let*

$$A = b_{12}b_{24} - b_{22}b_{14},$$

$$B = b_{11}b_{24} + b_{12}b_{23} - b_{13}b_{22} - b_{14}b_{21},$$

$$C = b_{11}b_{23} - b_{13}b_{21},$$

and

$$\begin{aligned}
P &= 2((b_{11} + b_{23})^2 - 2C) - (b_{12} + b_{24})^2, \\
Q &= ((b_{11} + b_{23})^2 - 2C)^2 - 2(b_{12} + b_{24})[(b_{11} + b_{23})B - (A + C)(b_{12} + b_{24})] \\
&\quad + 2(C^2 - A^2) - ((b_{11} + b_{23})(b_{12} + b_{24}) - B)^2, \\
R &= 2(C^2 - A^2)((b_{11} + b_{23})^2 - 2C) - 2B(A - C)[B - (b_{11} + b_{23})(b_{12} + b_{24})] \\
&\quad - [(A + C)(b_{12} + b_{24}) - (b_{11} + b_{23})B]^2, \\
S &= (C^2 - A^2)^2 - B^2(A - C)^2.
\end{aligned}$$

Let $u > 0$ be a constant which satisfies the equation

$$u^4 + Pu^3 + Qu^2 + Ru + S = 0 \quad (19)$$

The stationary solution loses its stability (γ is the bifurcation point) for the smallest positive γ given by

$$\gamma = \frac{1}{\sqrt{u}} \arccos \left(\frac{-B(A - (C - u)) + (b_{11} + b_{23})(b_{12} + b_{24})u}{A^2 - (C - u)^2 - (b_{11} + b_{23})^2u} \right). \quad (20)$$

Proof is in the Appendix 3.

In the next sections, for simplicity of calculations, our replicator system will be transformed into coordinates $x = n_1 = q_d n$ and $y = n$.

3.3.2 Numerical toolbox

Loss of the stability of rest points and the first bifurcation is the beginning of a very complex behavior. To analyze those events we use the numerical method from [67] to construct approximate solutions of Eqs. (33)-(35), using parameter values as in Section 2.3, while varying the delay γ in the range $\gamma \in [1, 50]$, with step size $\Delta\gamma \leq 10^{-2}$ (refined further in more chaotic regions). We start with a constant initial function for each value of γ and generate the solution $(n^\gamma(t), q_d^\gamma(t))$ over a long time interval. Since we are interested in the long-term behaviour of solutions (near the attractor), we discard the initial transients in the time range $t \in [-\gamma, S]$ for some fixed S . Then, for some $T \gg S$, we record all extrema of the solution $n(t)$, i.e., all points $t_i \in [S, T]$ such that $n'(t_i) = 0$. The value of T is chosen such that at least $N = 50$ extrema are identified. In cases where the solution tends toward a fixed point (for small values of γ), we record only one point. This type of diagram is commonly used in the study of bifurcations in DDEs; (see [68, 69], and references therein). The bifurcation diagram based on extrema, typically differs from bifurcation diagrams obtained from discrete maps like the logistic map or chaotic ODEs such as the Rössler system (see [71] and references therein). The concept of the extrema diagram relies on two observations: first, during a period-doubling bifurcation, a new extremum should appear in the diagram; and second, it is particularly useful when no natural candidate for a Poincaré section exists. While informative, some newly appearing periodic points in the extrema bifurcation diagram may be spurious i.e. not resulting from true bifurcations, but rather from small perturbations in the underlying solution, such as the so-called *kinks* [68]. Nevertheless, the emergence of these kinks typically precedes chaotic dynamics in DDEs (this method is used in section devoted to bifurcation analysis). All numerical trajectories are generated by JiTCODE delay differential equations solver for Python [73].

3.4 Derivation of the general framework for replicator dynamics with fertility delay resulting from the egg hatching or maturation time.

For simplicity, at this stage, consider uniform delays. Generalization to non-uniform delays for different strategies is the topic for the future research. To introduce delay to the fertility bracket we should renormalize the number of newborns per capita. If γ is the delay then we have

$$n_1(t - \gamma) e_1 V q^T(t - \gamma) \quad (21)$$

newborns. Then current per capita reproductive success is

$$\frac{n_1(t - \gamma)}{n_1(t)} e_1 V q^T(t - \gamma) \quad (22)$$

When we substitute this into the standard replicator equation we obtain the following fertility bracket in the replicator equation

$$\frac{n(t-\gamma)}{n(t)} [q_1(t-\gamma)V_1(t-\gamma) - q_1(t)\bar{V}(t-\gamma)]. \quad (23)$$

The above term is negative when:

$$q_1(t) > \frac{q_1(t-\gamma)V_1(t-\gamma)}{\bar{V}(t-\gamma)} = \frac{n_1(t-\gamma)V_1(t-\gamma)}{\sum_j n_j(t-\gamma)V_j(t-\gamma)}, \quad (24)$$

and the r.h.s of the above condition describes the frequency of the first strategy among newborns. The dynamics driven by the fertility bracket cannot escape the unit interval and for two strategies it reduces to:

$$[1 - q_1(t)] q_1(t-\gamma)V_1(t-\gamma) - q_1(t)(1 - q_1(t-\gamma))V_2(t-\gamma). \quad (25)$$

See Appendix 2 for detailed derivation.

Note that in this case background fertility rate Φ (which averaged over all strategies also equals Φ) will not vanish from replicator equations and will appear as the additional bracketed term:

$$\frac{n(t-\gamma)}{n(t)} [q_1(t-\gamma)\Phi - q_1(t)\Phi] \quad (26)$$

$$= \frac{n(t-\gamma)}{n(t)} [q_1(t-\gamma) - q_1(t)] \Phi. \quad (27)$$

It can be combined with fertility bracketed term. Therefore our system of replicator dynamics will have the following forms (newborns produced γ ago hatch from eggs and look for free nest sites). In a simplified form where V_1 and D_1 are demographic payoffs of the first strategy while \bar{V} and \bar{D} are average values:

$$\begin{aligned} \frac{dq_1}{dt} &= \frac{n(t-\gamma)}{n(t)} ([q_1(t-\gamma)V_1(t-\gamma) - q_1(t)\bar{V}(t-\gamma)] + [q_1(t-\gamma) - q_1(t)]\Phi) \\ &\quad - q_1(t) [D_1(t) - \bar{D}(t)] \end{aligned} \quad (28)$$

$$\frac{dn}{dt} = n(t-\gamma) [\bar{V}(t-\gamma) + \Phi] - n(t) [\bar{D}(t) + \Psi] \quad (29)$$

Note that for the delay $\gamma = 0$ the above system collapses to the equations (2,3). The expanded form of the above equations will be

$$\begin{aligned} \frac{dq_1}{dt} &= \frac{n(t-\gamma)}{n(t)} \left(\left[q_1(t-\gamma)e_1 V q^T(t-\gamma) - q_1(t) \sum_i q_i(t-\gamma)e_i V q^T(t-\gamma) \right] + [q_1(t-\gamma) - q_1(t)]\Phi \right) \\ &\quad - q_1(t) [(e_1 D q^T(t) - q(t) D q(t))] \\ \frac{dn}{dt} &= n(t-\gamma) \left[\sum_i q_i(t-\gamma)e_i V q^T(t-\gamma) + \Phi \right] - n(t) [q(t) D q(t) + \Psi] \end{aligned}$$

3.5 Density dependence

Now we should consider the problem of density dependent growth suppression. For the models without delay suppression can be realized by mortality acting on adult individuals. In this setting it does not affect the replicator dynamics (as in the standard models from textbooks). It can also act as the juvenile recruitment survival. This can be described by some multiplicative factor of fertility payoffs (for example logistic term $(1 - n/K)$, as in demographic models from [9, 10, 11]). Then replicator equation becomes sensitive for adult mortality factors acting on population size $n(t)$. This impact may lead to very complex dynamics such as in the case of periodic seasonal mortality or predator pressure. Introduction of delays complicates the problem even more. Since equation (28) depends on population size, due to factor $n(t-\gamma)/n(t)$, adult mortality factors may affect the dynamics of strategy frequencies even in the case without density dependent juvenile survival. If those factors are more complicated, such as seasonal mortality or predator pressure, the dynamics may be also complex.

Therefore, in this case we need some growth suppression factor acting on adult individuals, which will be present in the population size equation (29). We will use simple phenomenological linear mortality rate $\Omega n(t)$.

For juvenile survival the situation is also more complicated. We can use the standard logistic model $(1 - n(t)/K)$. Then the recruitment will be realized after maturation time (for example after egg hatching). The attracting point of the population size dynamics is

$$\tilde{n}(t) = \left(1 - \frac{[\bar{D}(t) + \Psi]}{[\bar{V}(t - \gamma) + \Phi]}\right) K, \quad (30)$$

If we want to use delayed juvenile survival, then we cannot simply use factor $(1 - n(t - \gamma)/K)$, as the obtained dynamics makes no sense in the following manner: the size $n(t)$ might be close to the limit K at a given t , while the dynamics accounts for the survival the value of $n(t - \gamma)$ in the past, which might be much smaller than K . In effect the population size may exceed K , changing the sign of the suppression bracket $(1 - n(t)/K)$. Which may lead to infinite population growth. This problem is known as Levins Paradox in the classical population models. Our model clearly shows that this is not a paradox but ordinary bug since frequency dynamics escapes the unit interval too. To counter this problem, for delayed recruitment, we might use some phenomenological decreasing fertility at birth (or egg laying time) described by multiplicative factor

$$u^{n(t-\gamma)/z} = e^{\frac{\ln(u)}{z}n(t-\gamma)}, \quad (31)$$

where $u \in (0, 1)$ and z is the scale parameter describing the population size where juvenile survival equals u . This factor should be rather interpreted as the density dependent fraction of eggs produced from the maximal potential, for example for some insect population.

3.6 Hawk-Dove game example

Derivation of the bracketed terms with (6) and (7):

$$\begin{aligned} & q_1(t - \gamma) e_1 V q^T(t - \gamma) - q_1(t) \sum_i q_i(t - \gamma) e_i V q^T(t - \gamma) \\ &= q_d^2(t - \gamma) 0.5F - q_d(t) 0.5F \\ &= (q_d^2(t - \gamma) - q_d(t)) 0.5F \end{aligned} \quad (32)$$

and for mortality bracket with (9) and (10) we have:

$$(e_1 d q^T(t) - q(t) d q(t)) = 0 - (1 - q_d)^2 0.5d \quad (33)$$

When we substitute the payoff functions of the Hawk-Dove game to equations (28,29) we obtain the system of equations:

$$\begin{aligned} \frac{dq_d}{dt} &= \frac{n(t - \gamma)}{n(t)} [q_d^2(t - \gamma) - q_d(t)] 0.5F \mathbf{D}(n(t)) + \\ &\quad \frac{n(t - \gamma)}{n(t)} [q_d(t - \gamma) - q_d(t)] \Phi \mathbf{D}(n(t)) + q_d(t) (1 - q_d(t))^2 0.5d \end{aligned} \quad (34)$$

$$\frac{dn}{dt} = n(t - \gamma) (0.5F + \Phi) \mathbf{D}(n(t)) - n(t) \left[(1 - q_d(t))^2 0.5d + \Psi + \mathbf{A} + \mathbf{B} + \mathbf{C} \right] \quad (35)$$

$$\frac{dx}{dt} = x(t) b_p n(t) - x(t) d_p \quad (36)$$

where juvenile survival $\mathbf{D}(n(t))$ will have following variants:

- a) $\mathbf{D}(n(t)) = 1$ lack of density dependent juvenile mortality factors;
- b) $\mathbf{D}(n(t)) = \left(1 - \frac{n(t)}{K}\right)$ logistic suppression, after maturation period every juvenile individual can check single random nest site. If it will be free it will survive and will be successfully recruited;
- c) $\mathbf{D}(n(t)) = u^{n(t-\gamma)/z}$ recruitment with the delay, where $u \in (0, 1)$ and z is the scale parameter describing the population size where juvenile survival equals u ;

The rest of the optional adult mortality factors will be:

A = $\alpha (1 + \sin(\frac{2\pi}{\theta}t))$ seasonal fluctuations of the background mortality, where α describes amplitude and θ duration of the season;

B = $px(t)$ impact of predators;

C = $\Omega n(t)$ phenomenological linear adult density dependent mortality;

Note that, for zero delays and logistic juvenile survival the above system reduces to (11,12).

4 Numerical simulations

4.1 Case without juvenile recruitment mortality, type a) juvenile survival

Let us consider the version of the model with $\mathbf{D}(n(t)) = 1$. In this case we need to suppress the unlimited exponential growth by linear density dependent adult mortality of type **C** which is $\Omega n(t)$. Figure 1 shows the trajectories of the model with the delay $\gamma = 15$ and for the parameters $F = 0.9$, $d = 1$, $\Phi = 0.5$, $\Psi = 0.2$ and $\Omega = 0.0001$. The initial history is constant and equals $q_d = 0.8$ and $n = 100$. This case is equivalent to the classical textbook replicator dynamics, the only difference is the introduction of the delay. However, as we can see in Figure 1 the dynamics is more sophisticated showing small scale oscillations and the overshoot of the equilibrium.

The trajectories are very sensitive for initial histories. This is shown in Figure 2 where the initial frequency linearly grows from 0.35 to 0.8 and the population size declines linearly from 3100 to 100. This situation can be interpreted as the rapid ecological catastrophe where Hawks suffered greater mortality than Doves. As we can see trajectories are dramatically different than for the constant history.

Without delay the standard textbook replicator dynamics is closed and nothing can affect the dynamics of the strategy frequencies. We can see that in the case of the model with the delay in fertility payoffs, this is not the case anymore even without additional density dependent juvenile recruitment mortality. When we add some periodic mortality (additional adult mortality of type **A** with amplitude $\alpha = 0.2$ and period $\theta = 120$) we can observe induced oscillations of the strategy frequencies in addition to the oscillations of the population size (Fig. 3).

Similar behaviour we can observe when we add to our model additional equation and mortality factor describing the predator pressure. In effect we obtain combination of the replicator dynamics and simple Lotka-Volterra system. The parameters of the prey-predator subsystem are $b_p = 0.3$, $d_p = 0.8$ and $p = 0.6$. In this case instead of external oscillator, we have additional feedback. Trajectories are depicted in Fig. 4 and phase portraits in Fig. 5. When we combine the predator pressure with seasonal mortality (with amplitude $\alpha = 0.25$ and period $\theta = 120$), the resulting cycling behaviour is even more complex (see Fig. 6 and 7).

4.2 Case with the logistic juvenile recruitment mortality, type b) juvenile survival

This is the model similar to the previous works on demographic games [9, 10, 11], but with added delay. Model parameters are $F = 1.7$, $d = 1$, $\Phi = 0.5$, $\Psi = 0.2$ and the delay $\gamma = 15$. We assume the non constant history, frequency declining from 0.225 to 0.05 and the population size declining from 560 to 260. Numerical simulations show that when trajectory reaches the neighbourhood of the area limited by nullclines, then the fluctuations resulting from the delay disappear and the system behaves similarly to the model without delay (Fig 8). This may be result of the slowdown of the pace of convergence in the area limited by nullclines. In effect, impact of the delay is weaker due to smaller differences in the values of the population state at time t and $t - \gamma$.

When we replace the constant background mortality by seasonal mortality fluctuating around the same value by setting $\Psi = 0$ and adding $\alpha = 0.25$ and period $\theta = 120$, we observe the overshoot of the intersection and the limit cycle is significantly above it (Fig. 9).

We also can combine our model with predator impact for parameters $F = 0.7$, $d = 1$, $\Phi = 2$, $\Psi = 0.2$, carrying capacity $K = 50$ and with delay $\gamma = 15$. We change initial history where frequency declines linearly from 0.95 to 0.05 and population size linearly increases from 1.5 to 3. Initial number of predators equals 2. Parameters for the predator subsystem are again $b_p = 0.3$, $d_p = 0.8$ and $p = 0.6$. The obtained cyclic trajectories are very sophisticated (Fig. 10 and Fig. 11). We obtain an interesting pattern, when we replace the constant mortality with periodic mortality by setting $\Psi = 0$ and amplitude $\alpha = 0.4$ and period $\theta = 12$. Seasonality do not alters the frequency dynamics significantly, but surprisingly induces greater oscillations on the predator population (Fig. 12 and 13).

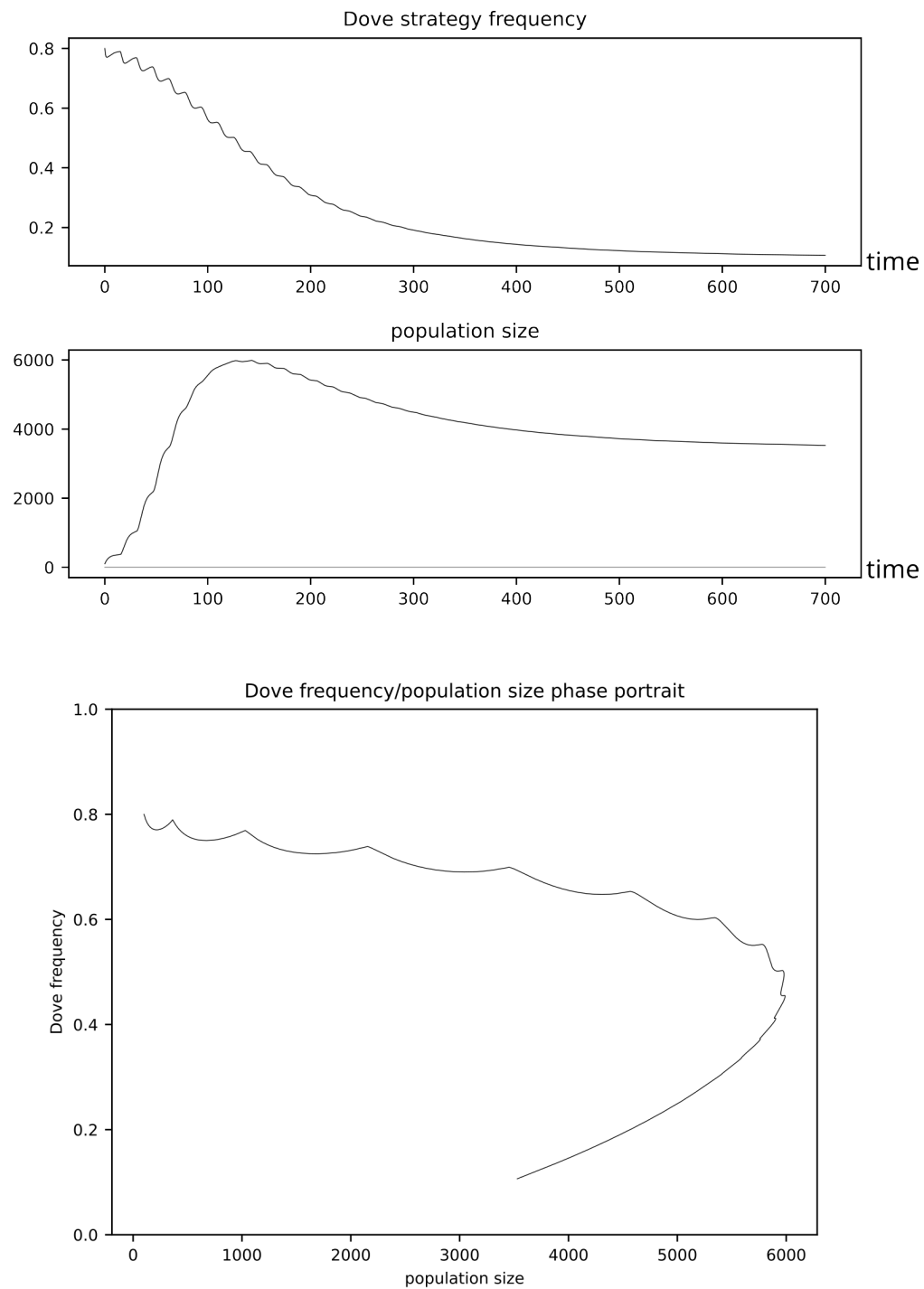


Figure 1: Case without juvenile mortality factors. Trajectory for parameters $F = 0.9$, $d = 1$, $\Phi = 0.5$, $\Psi = 0.2$ and $\Omega = 0.0001$ and the constant initial history $q_d = 0.8$ and $n = 100$.

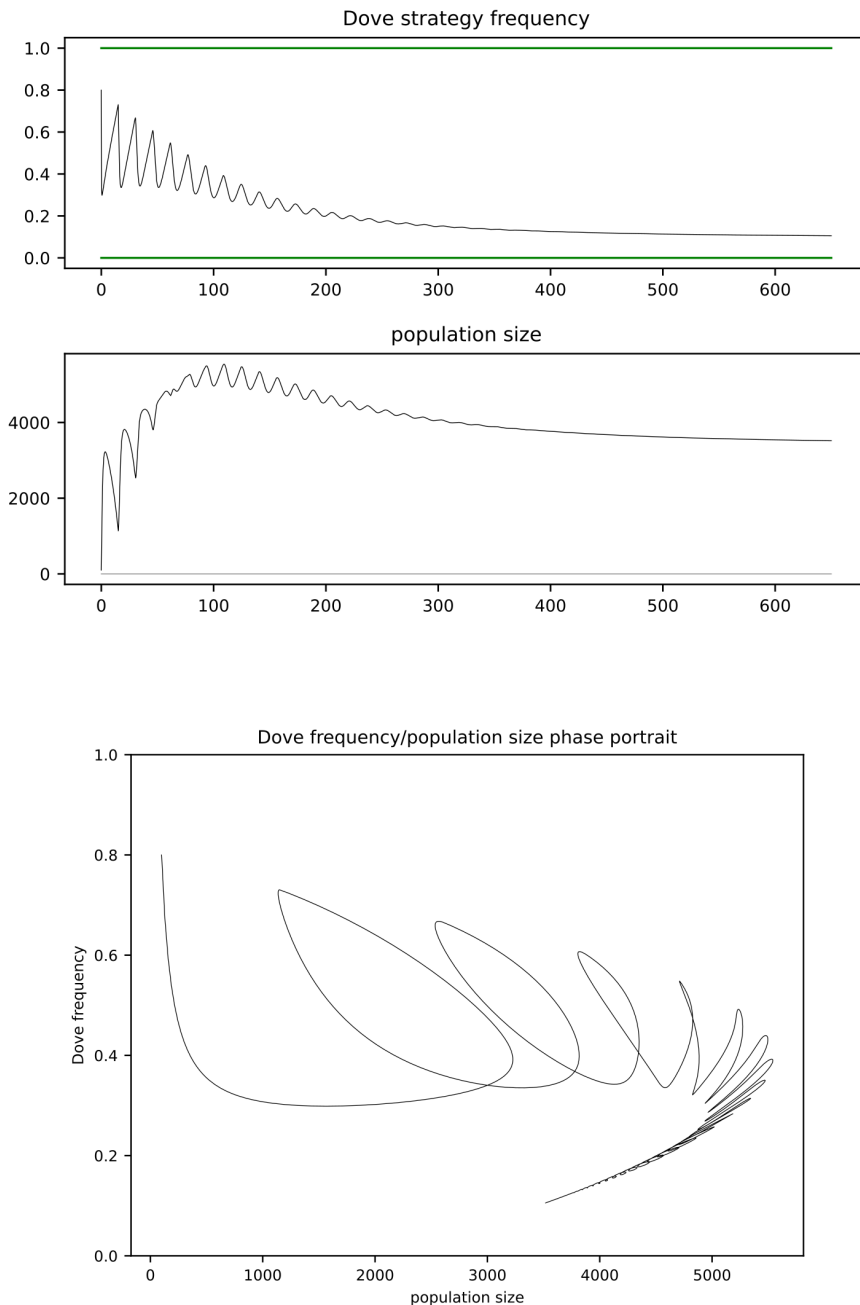


Figure 2: Case with non-constant initial history. Initial frequency linearly grows from 0.35 to 0.8 and the population size declines linearly from 3100 to 100.

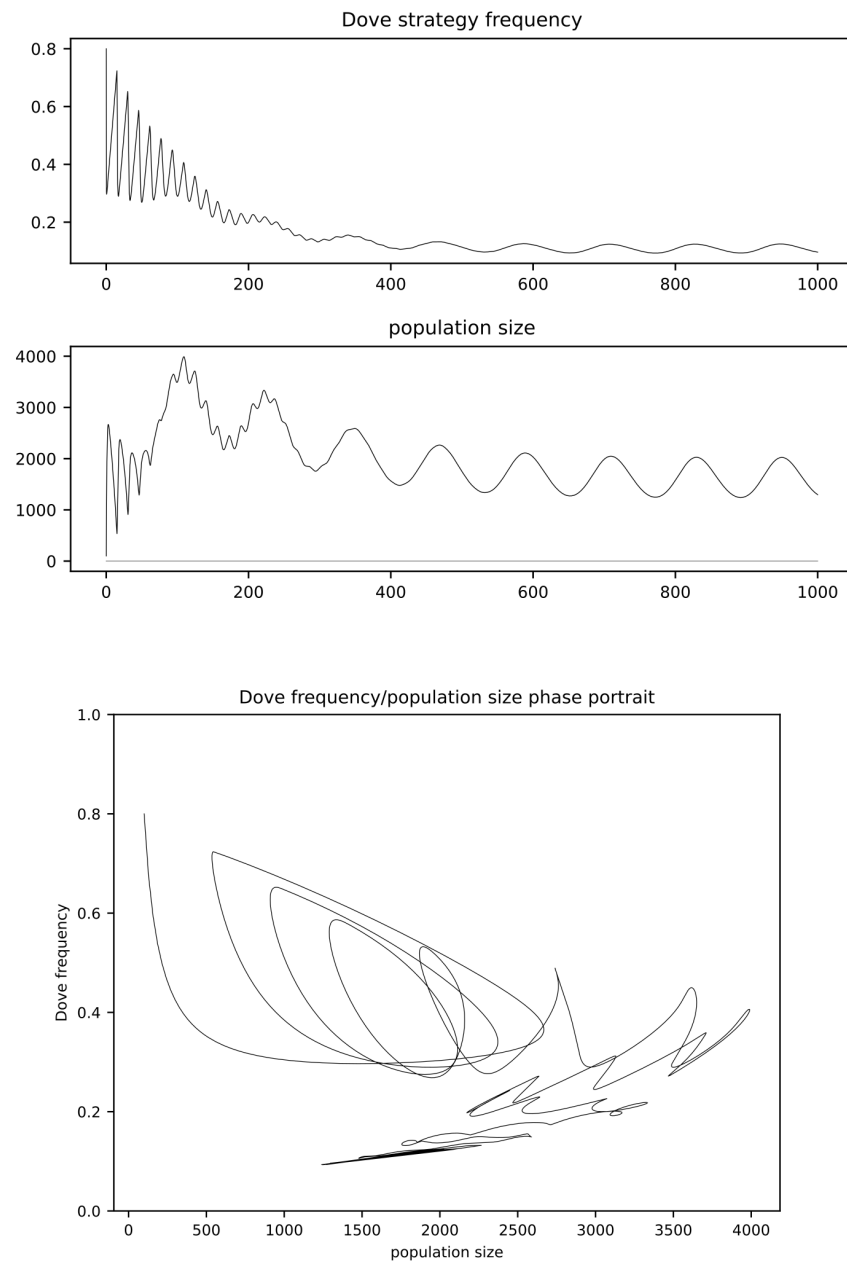


Figure 3: Trajectories with added periodic background mortality with amplitude $\alpha = 0.2$ and period $\theta = 120$.

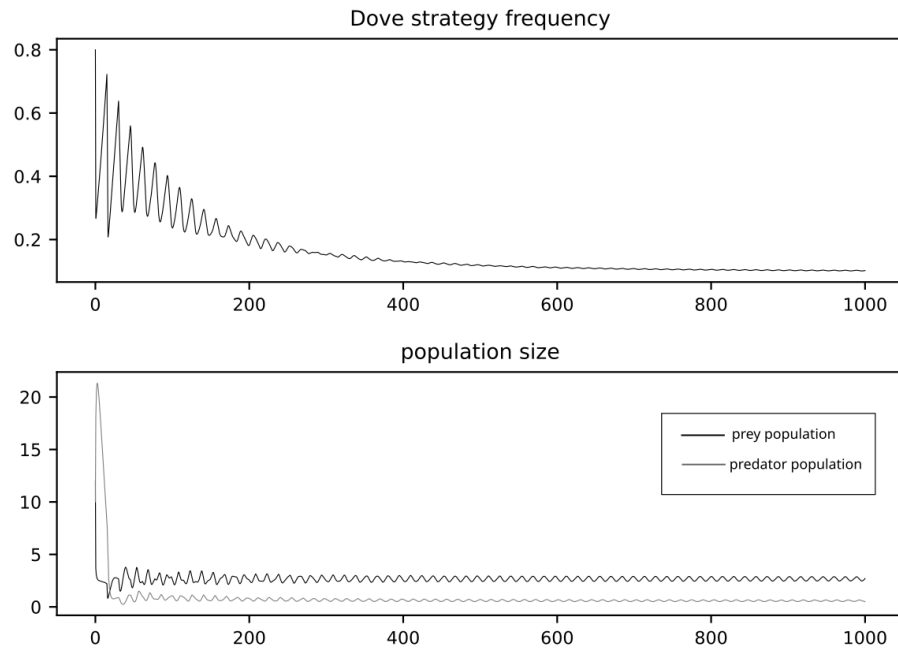


Figure 4: Case with added predator pressure. Parameters of the predator-prey subsystem are $b_p = 0.3$, $d_p = 0.8$ and $p = 0.6$.

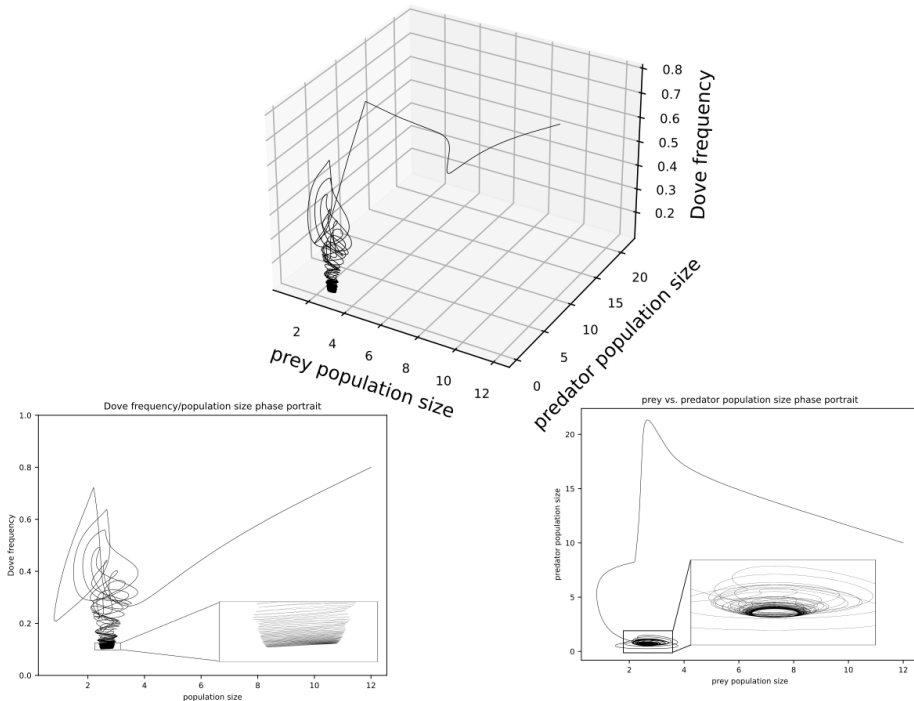


Figure 5: Phase portraits of the system from Fig.4

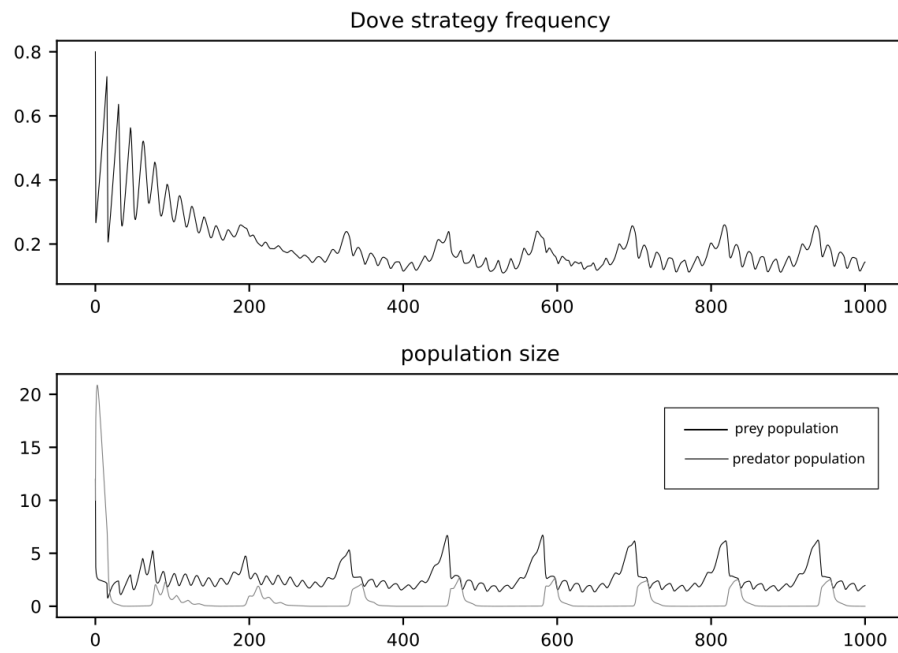


Figure 6: System with predator pressure from Figure 5 with additional seasonal mortality (with amplitude $\alpha = 0.25$ and period $\theta = 120$)

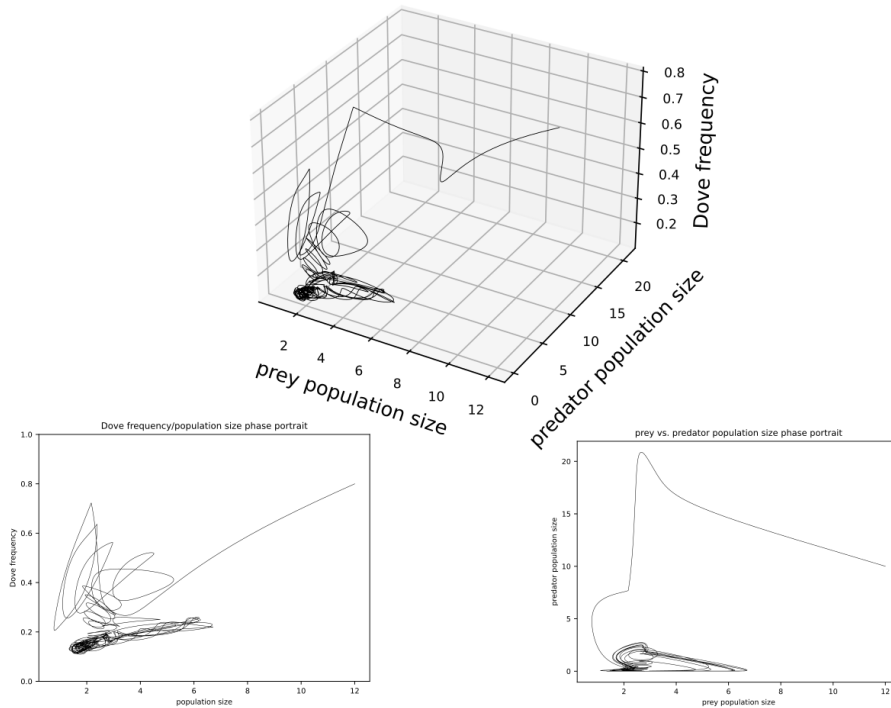


Figure 7: Phase portraits of the system from Fig.6.

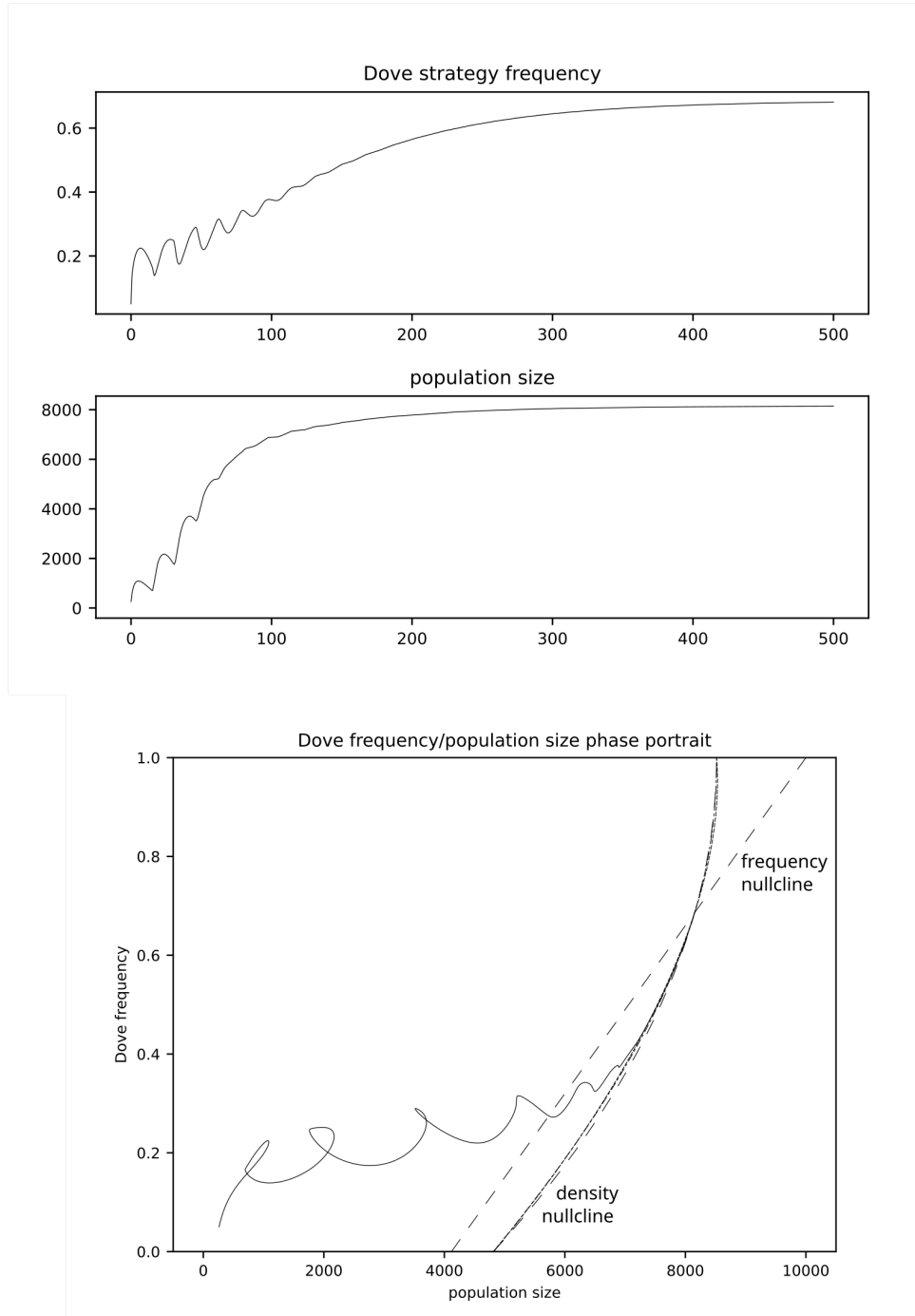


Figure 8: Model with logistic juvenile recruitment survival. Parameters are $F = 1.7$, $d = 1$, $\Phi = 0.5$, $\Psi = 0.2$ and the delay $\gamma = 15$. We assume the non constant history, frequency declining from 0.225 to 0.05 and the population size declining from 560 to 260. Nullclines are shown in dashed lines.

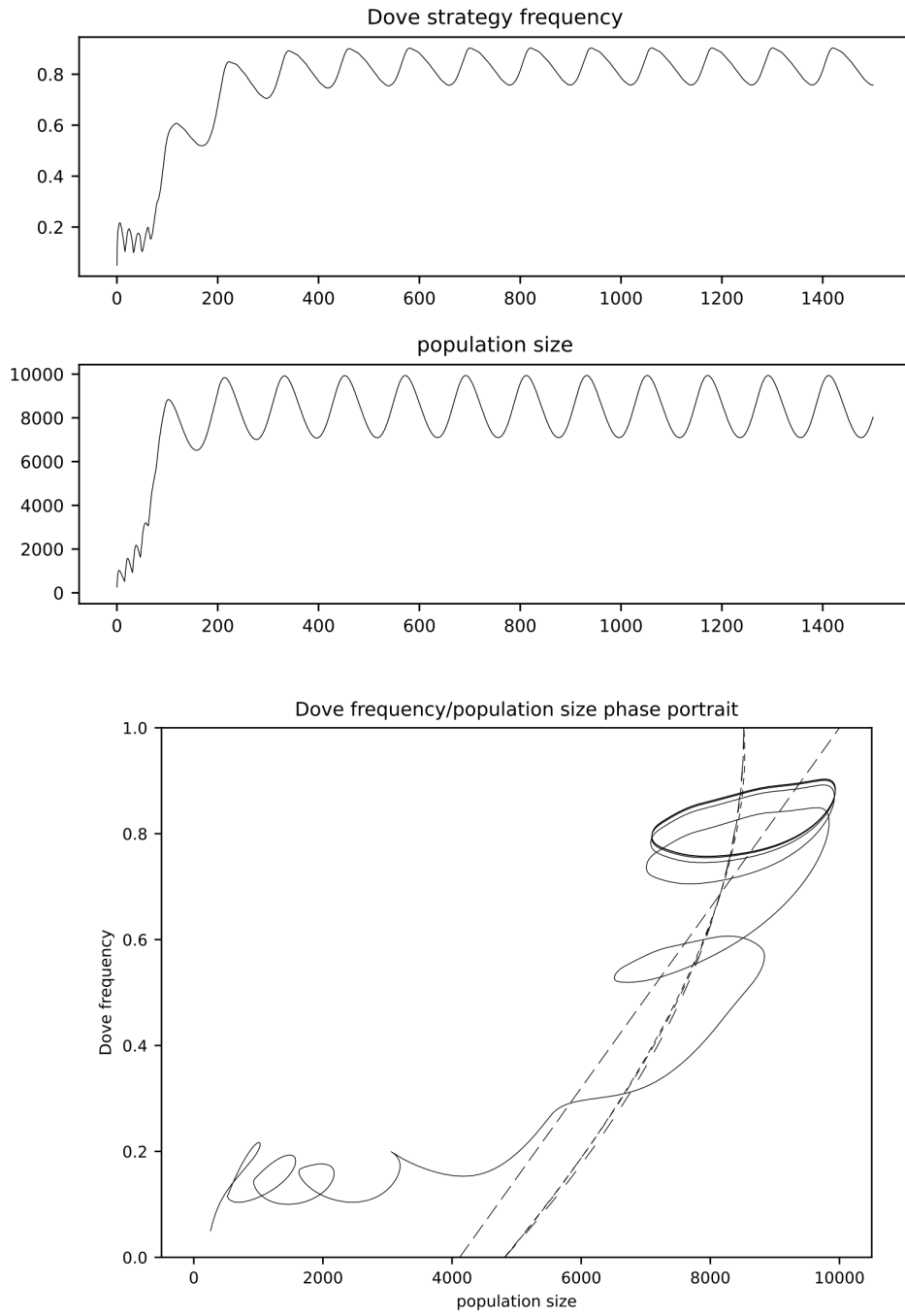


Figure 9: Model from Fig.8 with constant background mortality replaced (by setting $\Psi = 0$) by periodic mortality with amplitude $\alpha = 0.4$ and period $\theta = 12$. We can observe the overshoot of the intersection of the nullclines (dashed lines).

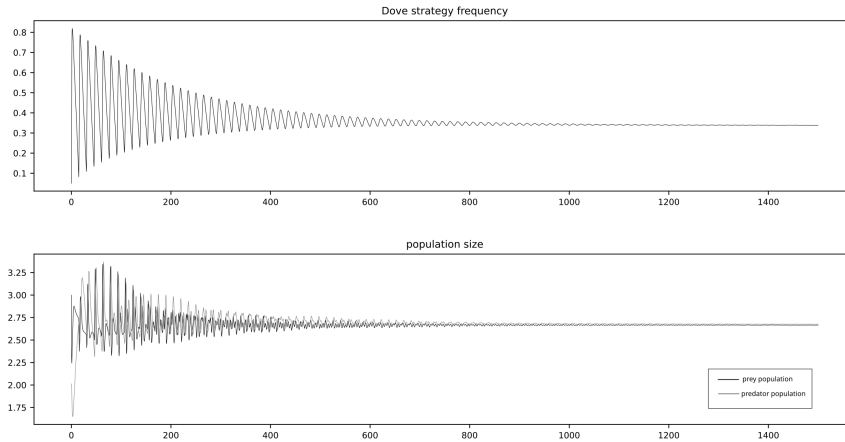


Figure 10: Model with added predator pressure. Parameters are $F = 0.7$, $d = 1$, $\Phi = 2$, $\Psi = 0.2$, carrying capacity $K = 50$ and with delay $\gamma = 15$. Parameters for the predator subsystem are $b_p = 0.3$, $d_p = 0.8$ and $p = 0.6$. Initial history where frequency declines linearly from 0.95 to 0.05 and population size linearly increases from 1.5 to 3.

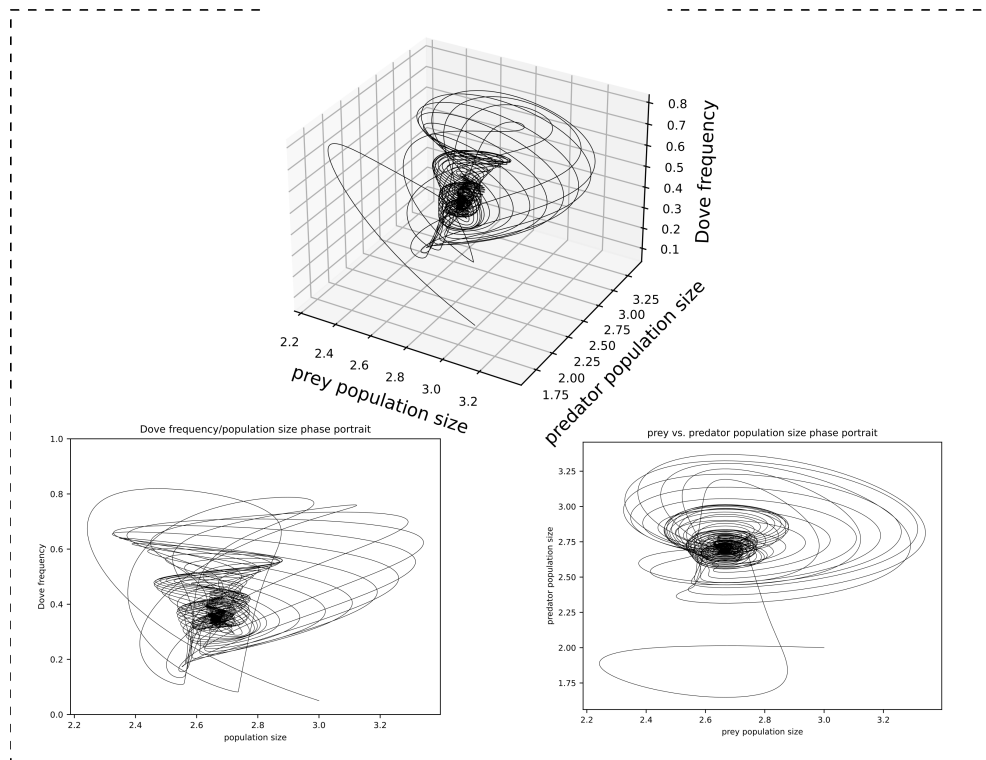


Figure 11: Phase portraits of the system from Fig. 11.

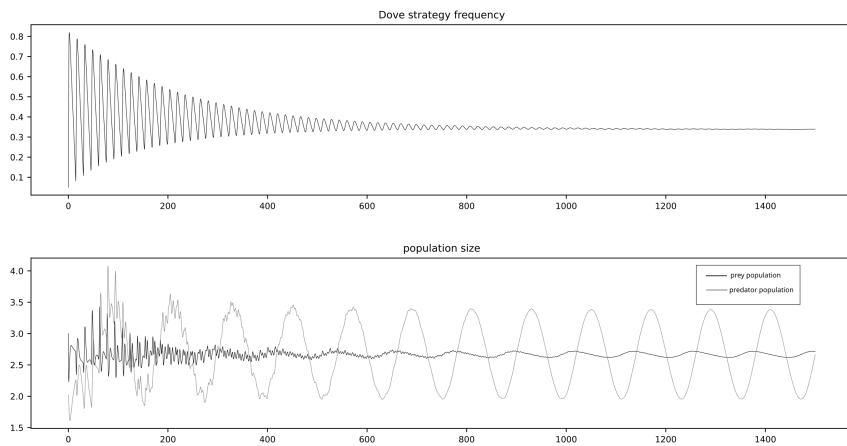


Figure 12: System from Figures 10 and 11 with replaced constant mortality with periodic mortality by setting $\Psi = 0$ and amplitude $\alpha = 0.4$ and period $\theta = 12$.

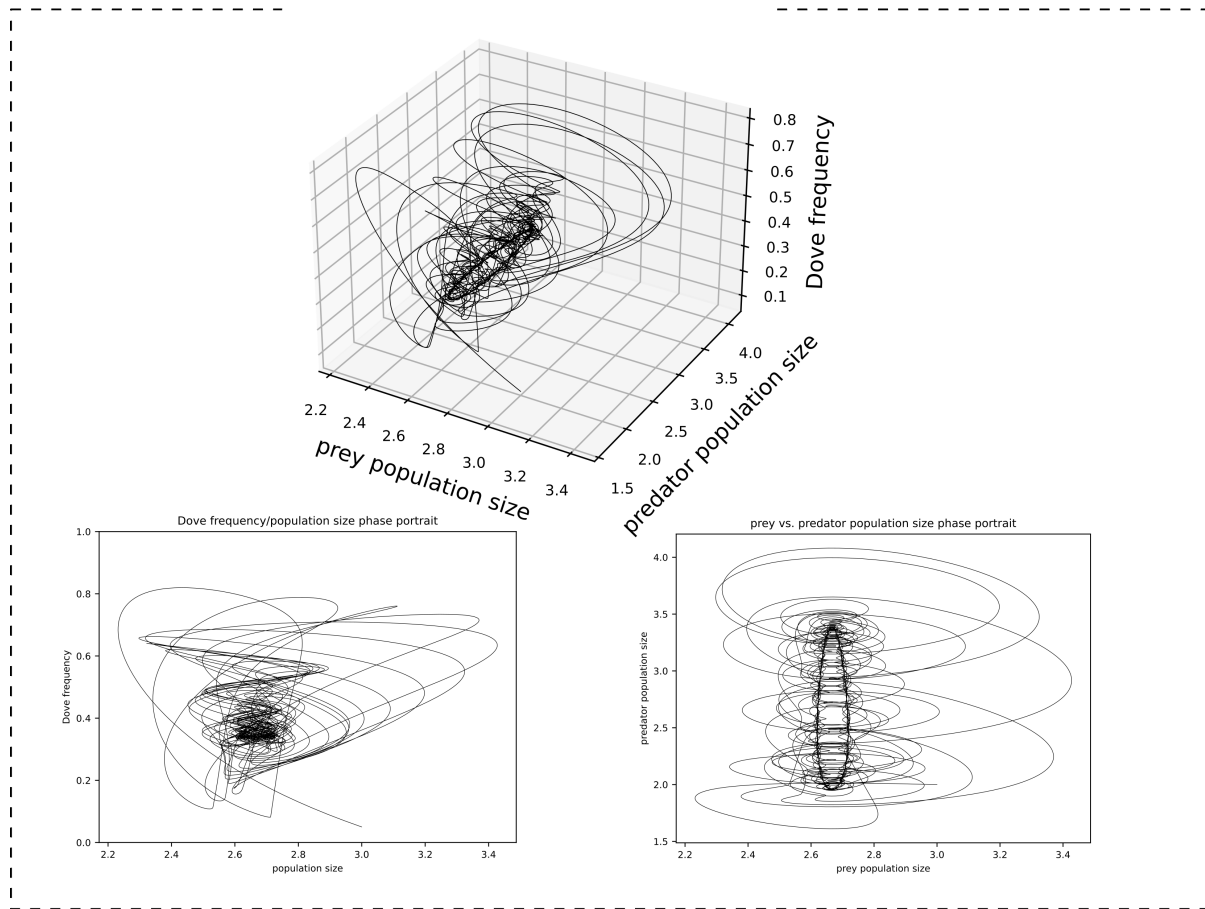


Figure 13: Phase portraits of the system from Fig. 11.

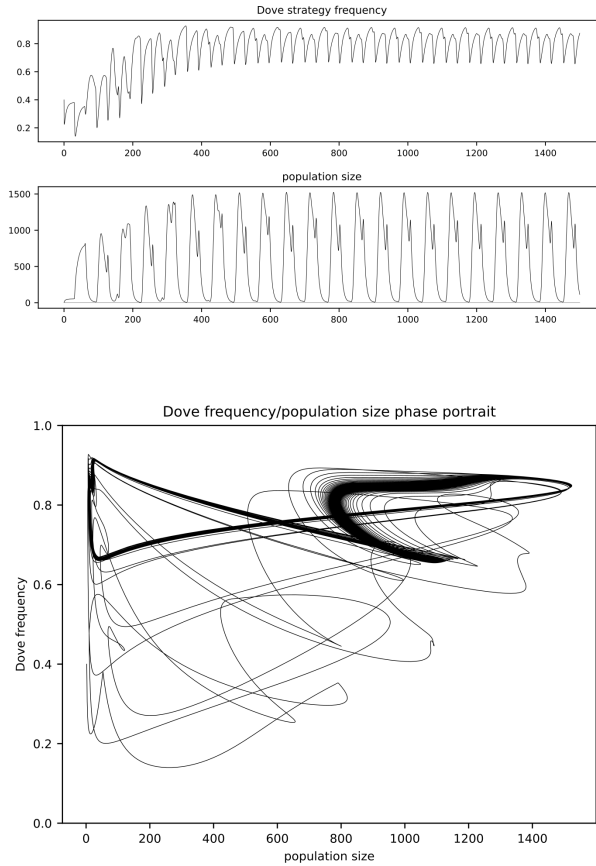


Figure 14: Model with delayed juvenile recruitment $\mathbf{D}(n(t)) = u^{n(t-\tau)/z}$ with parameters $u = 0.6$ and $z = 50$. Payoff parameters are $F = 18$, $d = 1$, $\Phi = 0.5$, $\Psi = 0.158$ and delay $\gamma = 30$. Constant history with frequency 0.4 and populations size 2. We can observe bifurcation leading to the complex cycle, forming the Elvis-Presley-shaped pattern.

4.3 Case with the delayed juvenile recruitment mortality, type c) juvenile survival

Figure 14 shows the resulting complex cyclic trajectories. This version of the model is very sensitive to small changes of the parameters.

In the case of delayed juvenile recruitment $\mathbf{D}(n(t)) = u^{n(t-\gamma)/z}$ we can observe the cascade of bifurcations. Let us set the parameters $F = 18$, $d = 1$, $\Phi = 0.5$, $\Psi = 0.158$, parameters of juvenile survival function are $u = 0.6$ and $z = 50$ and delay $\gamma = 30$. Initial history is constant with frequency 0.4 and populations size 2.

For example when we set the background mortality for $\Psi = 0.184$ we can obtain even more complex patterns (Fig. 15). We can set the significantly greater delay $\gamma = 394.7$. Since single time unit is the average per capita time between interactions, this long delay is biologically plausible for long living organisms. In this example we want to show maximal complexity of the obtained trajectories, which are depicted in Fig. 16 and Fig. 17.

It is interesting, what happens when we divide the background mortality into the constant and the fluctuating part by setting $\Psi = 0.008$ and for fluctuating part the amplitude $\alpha = 0.4$ and period $\theta = 12$. The obtained trajectories show extreme impact on the dynamics of strategy frequencies (Fig. 18 and Fig. 19).

Adding the predator pressure modelled by simple Lotka-Volterra system leads to the similar behaviour than in the case of logistic juvenile survival without delay. Therefore presenting it in detail is pointless.

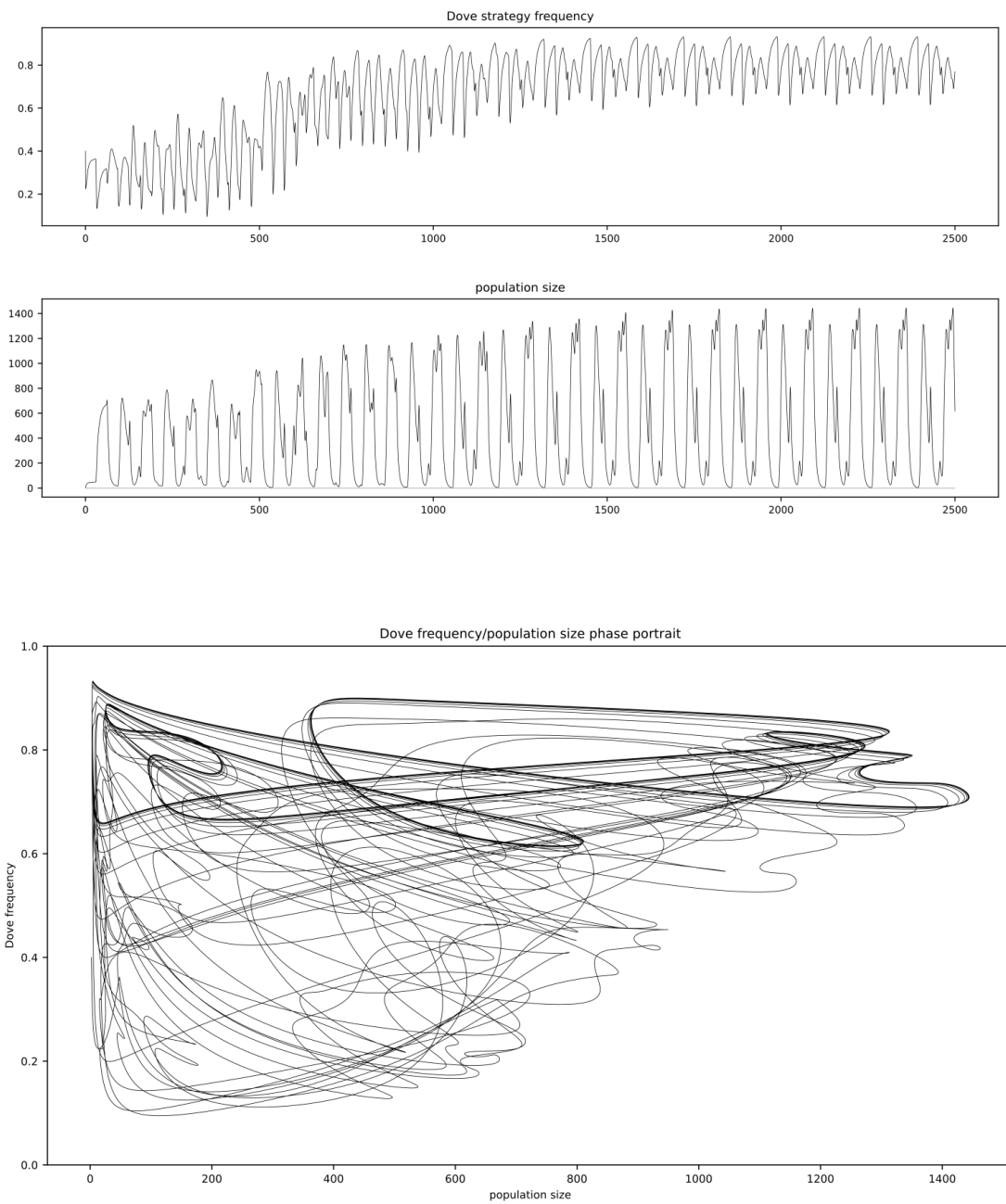


Figure 15: Model from Fig.14 with only altered background mortality $\Psi = 0.184$. We can observe dramatical increase in complexity of trajectories.

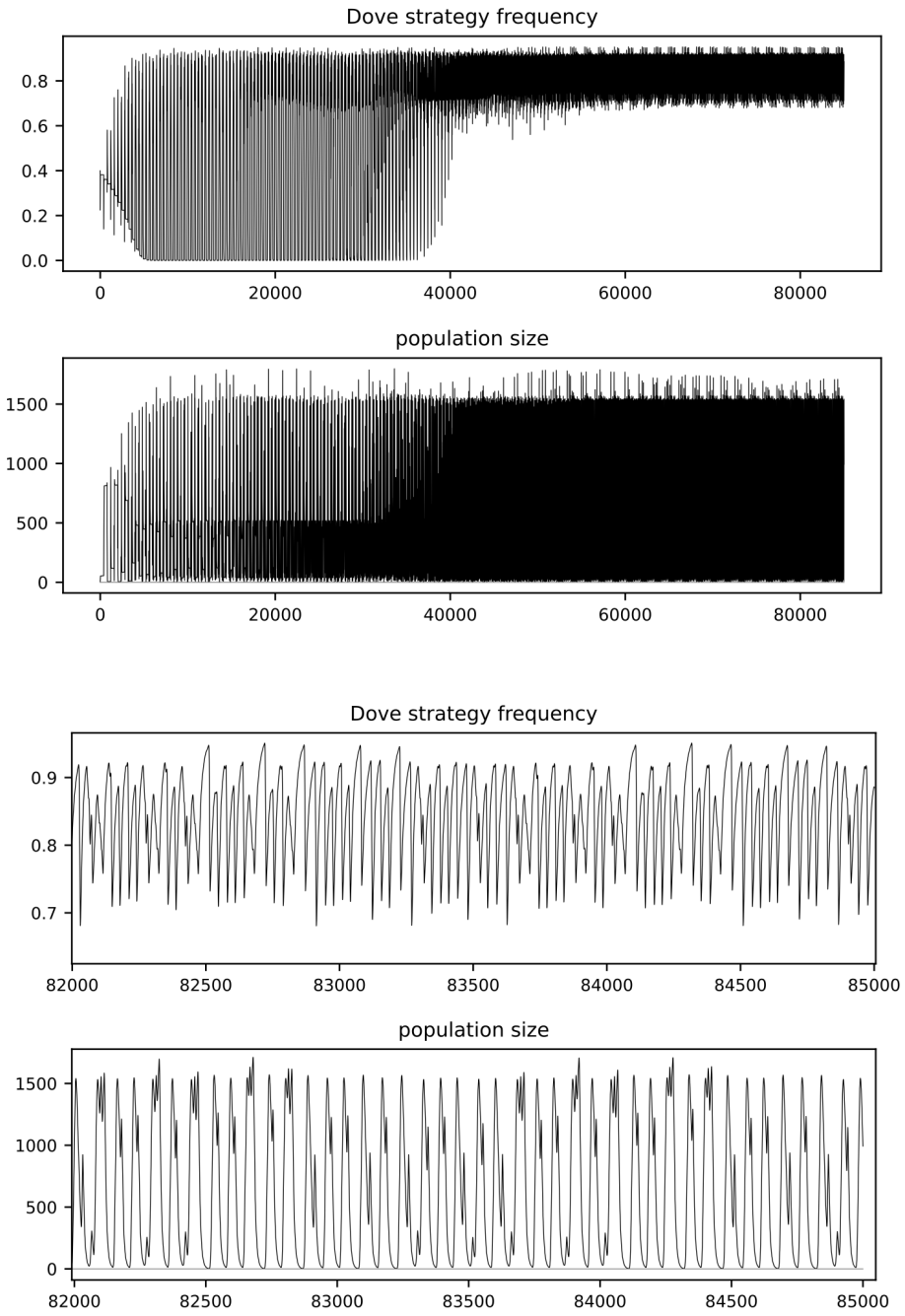


Figure 16: System from Fig. 15 with long delay $\gamma = 394.7$. Long transient leading to the rapid regime shift can be observed. The underlying mechanism remains unknown, and suggests possible route for a future research.

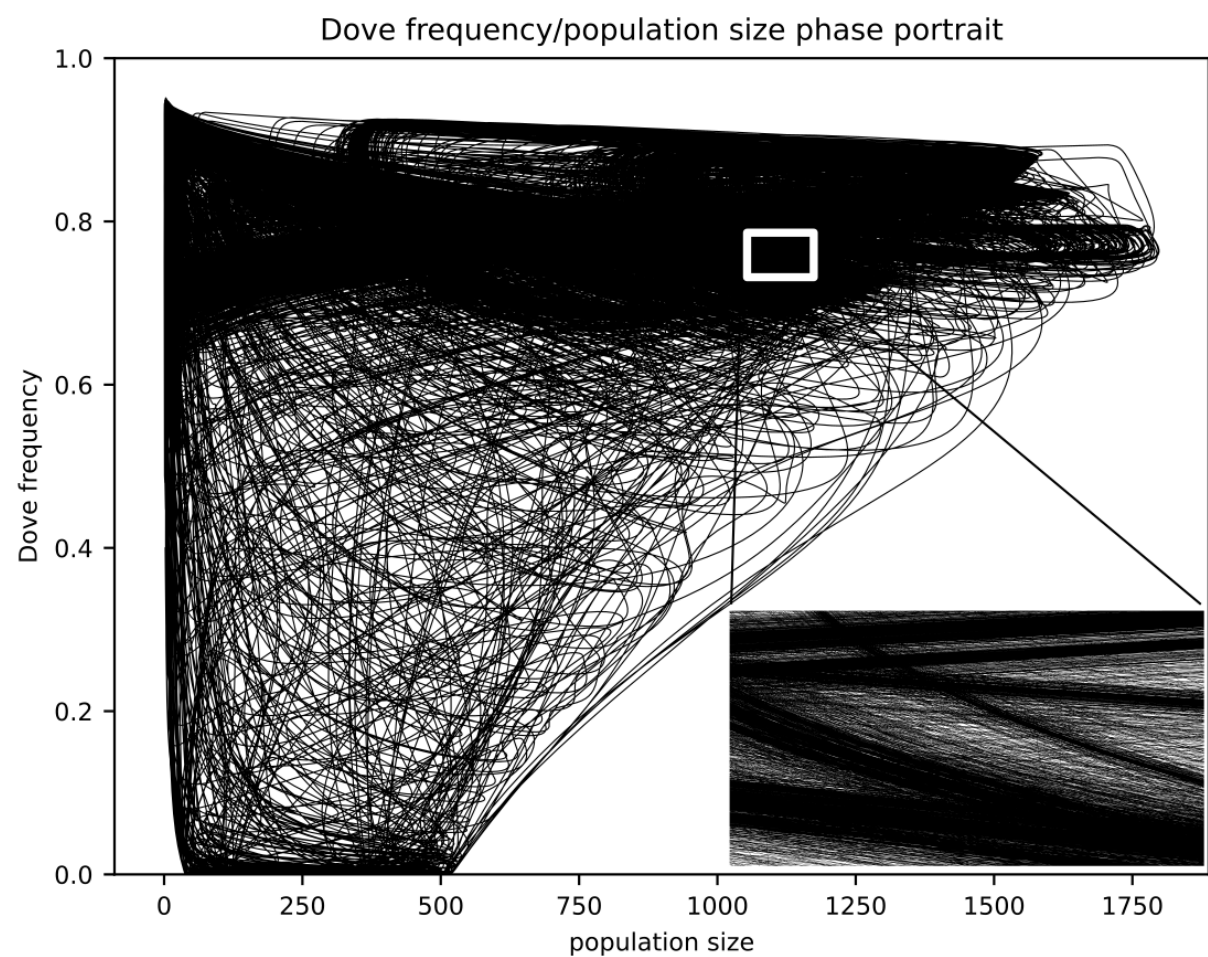


Figure 17: Phase portrait for the system from Fig. 16.

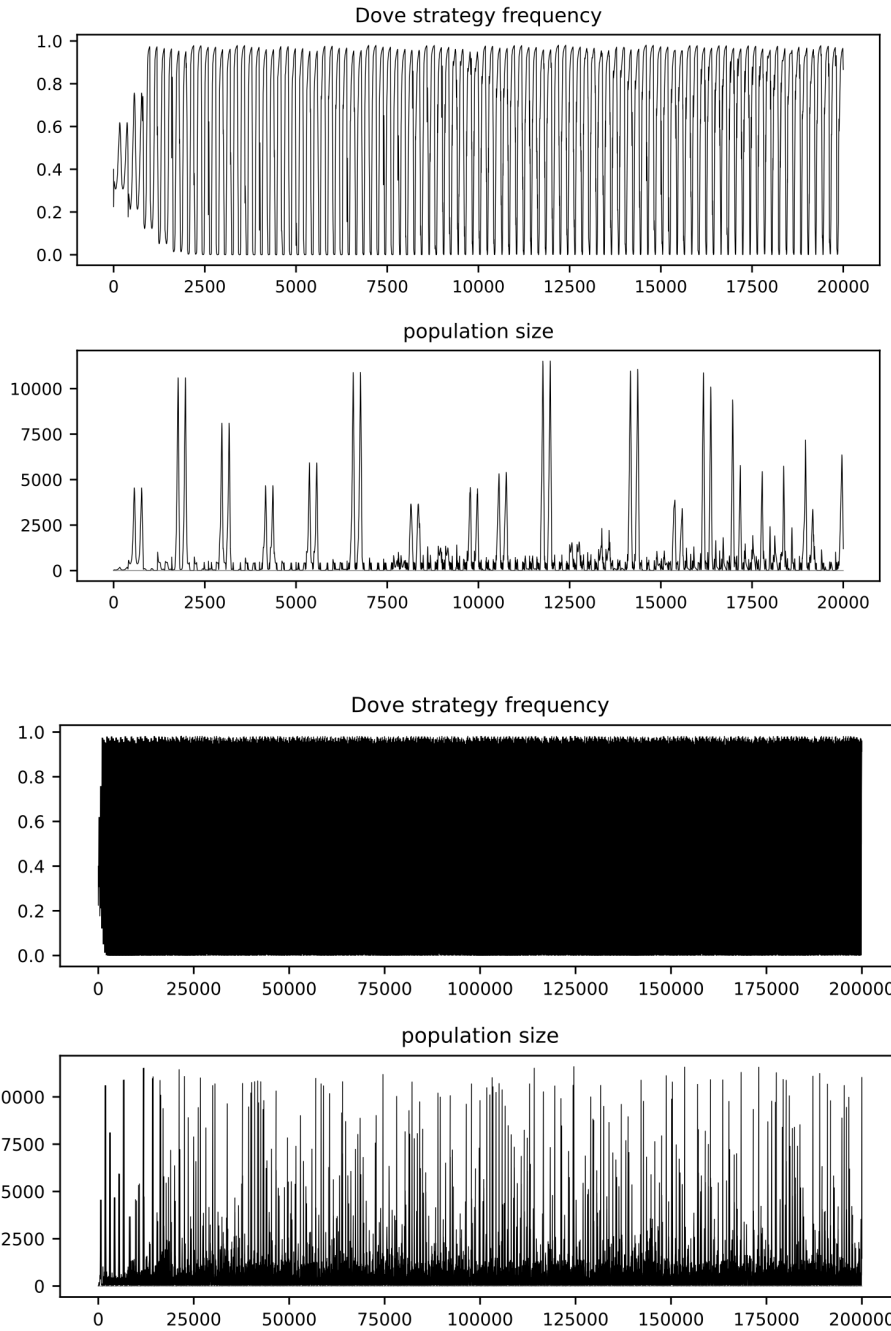


Figure 18: System from Fig. 16 and 17 with added periodic mortality by setting mortality $\Psi = 0.008$ and for fluctuating part the amplitude $\alpha = 0.4$ and period $\theta = 12$. We can observe that mechanism of the strategic selection is completely inefficient. In addition, the ecological dynamics shows the "boom and bust" pattern.

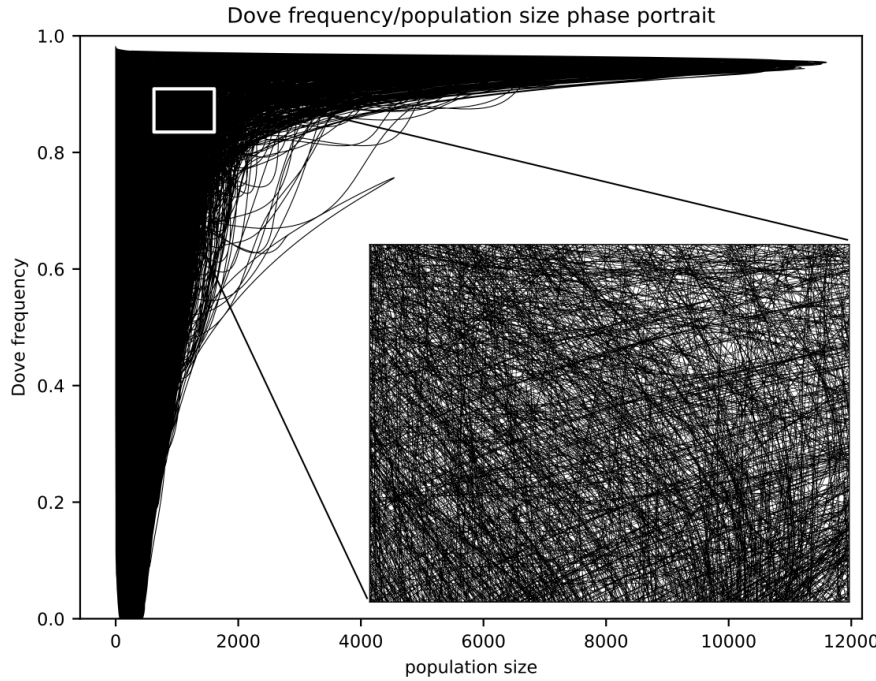


Figure 19: Phase portrait for the system from Fig 18.

4.4 Bifurcation analysis

The parameters of systems with density dependence driven by adult mortality or logistic juvenile recruitment survival in a long run generate very simple dynamics (steady states and periodic orbits under seasonality), therefore we do not present bifurcation diagrams for those. We start from the application of the Theorem 1 and present a plot of the surfaces of the first bifurcation and the loss of stability of the stable point as the functions of the model parameters (F , d and Φ , Ψ , see Figure 20). The simplification of the system and derivation of the respective coefficients is in the Appendix 4. The plots are obtained numerically by simple algorithm: firstly, checking that the rest point exists and choosing the smallest positive root of the characteristic polynomial (if it exists). The Scilab source code is available in Supplementary Materials and in repository [81].

As we can see, for certain parameter values the equilibrium point may be not affected by delays, while for another it may lose stability in effect of bifurcation. Thus the question arises, what happens for even longer delays than the critical bifurcation value? We can analyze the bifurcation structure for the interesting case when the initial bifurcation avoids the extinction of the Dove strategy. The extreme values $n_i^\gamma = n^\gamma(t_i)$, indicating bifurcations, are plotted in Figure 21 against the corresponding γ . We also present the corresponding values $q_{d,i}^\gamma = q_d^\gamma(t_i)$ in the lower panel of Fig. 21. The system parameters, time values S , T , and the number of points N are provided in the accompanying source codes [70]. Interested readers may use those codes to recompute the bifurcation diagrams presented in this paper. In what follows, we present the orbits in the standard $(u(t), u(t - \gamma))$ projection in Figures 22–29, which is suitable for visualizing periodic motion, as periodic solutions appear in these coordinates as closed loops. Several interesting events occur on the route to chaos in this system. The first Hopf bifurcation takes place in region 1, for $\gamma \in [2.3, 2.7]$ (exact value computed according to Theorem 1 is $\gamma = 2.5147879$). The steady state loses stability and a periodic orbit in $n(t)$ emerges, see Fig. 22. Then, for some $\gamma \in [4.260, 4.265]$, there is an abrupt change in dynamics, resulting in the emergence of a closed cycle in q_d and a shift in the trajectory of n . A more detailed analysis of this bifurcation is necessary but lies outside the scope of the present paper. For larger γ , the picture becomes more complex; many of the appearing, disappearing, and intersecting curves are caused by *kinks* and/or are artefacts of the extrema-based bifurcation diagram, as discussed earlier; see Figures 24 and 25. Period-doubling bifurcations are also observed, as shown in Fig. 26. These eventually lead to the onset of chaos for values of $\gamma \in [39.2, 39.6]$. The stability regions, such as region 10, feature complex attracting periodic orbits, typical in systems with unimodal feedback (see, e.g., [72]). This suggests the presence of many additional structures, such

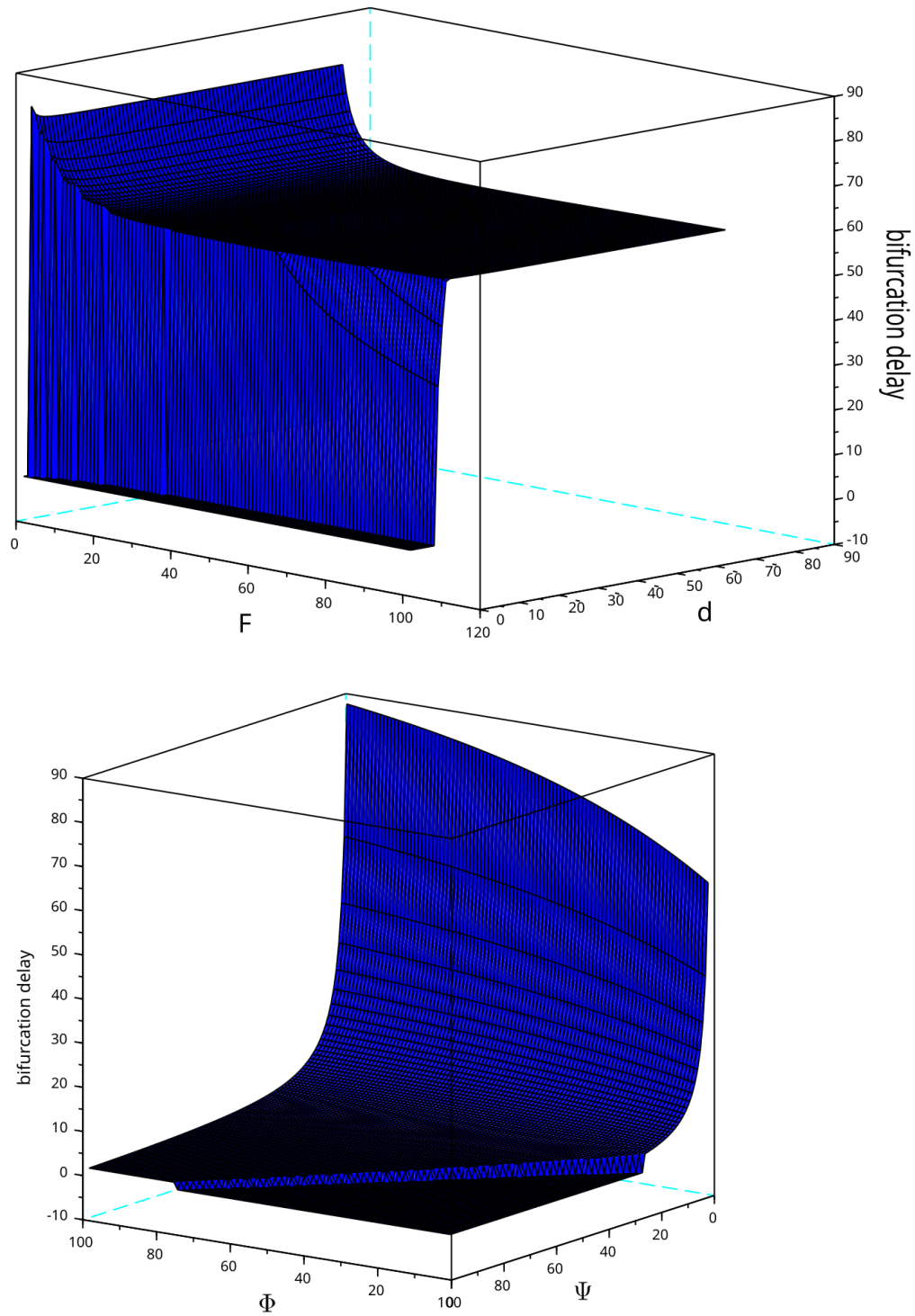


Figure 20: Plot of the bifurcation surfaces resulting from the application of the Theorem 1. Panel a) shows the plot over values of the focal game parameters F and d for fixed values $\Psi = 0.0115$ and $\Phi = 0.1$. Panel b) shows the plot over values of the background parameters Φ and Ψ for fixed values $F = 0.6$ and $d = 1$

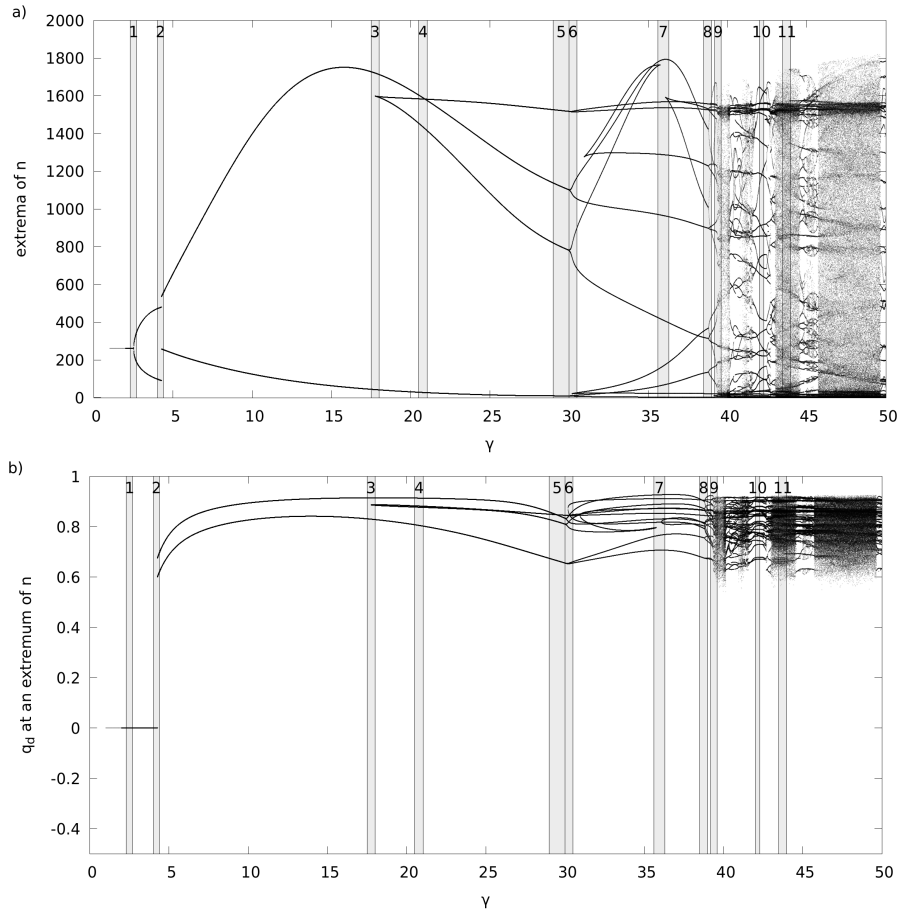


Figure 21: An extrema bifurcation diagram for Dove system with third kind of $D(n(t))$ function. For each value of γ we record all extrema of the function $n(t)$ (i.e. values $n(t_i)$ where $n'(t_i) = 0$) after the numerical solution approaches the apparent attractor. The values of q_d are recorded at the same points t_i . The grey bars numbered 1–11 corresponds to the plots discussed in Section 4.4

as an infinite number of unstable periodic orbits (see, e.g., [71]). Finally, in Fig. 29, we show data from the chaotic region 11, where the dynamics closely resembles those observed in classical equations such as the Mackey-Glass or Lasota-Wazewska systems.

4.5 Long transients are even longer under delay

In the previous section we observed that the classical rest points under juvenile recruitment with delay can be highly sensitive to the impact of the delay. In this section we examine the performance of "ghost attractors" responsible for the long transient behavior. "Ghost attractors" emerge after a saddle-node bifurcation, when the nullcline intersections collide and disappear. Then nullclines disconnect and form a narrow channel, still attracting the trajectories and catching them for some time. In our Hawk-Dove model this happens when Δ is negative but still very close to zero. We observe the paradoxical effect that the classical rest points are very fragile with respect to the impact of delays while ghost attractors (objects that do not exist from the point of view of the classical theory) are getting stronger and their duration increases with the delay. This is depicted in Figure 30 for the short delays and in Figure 31 for the very long delays.

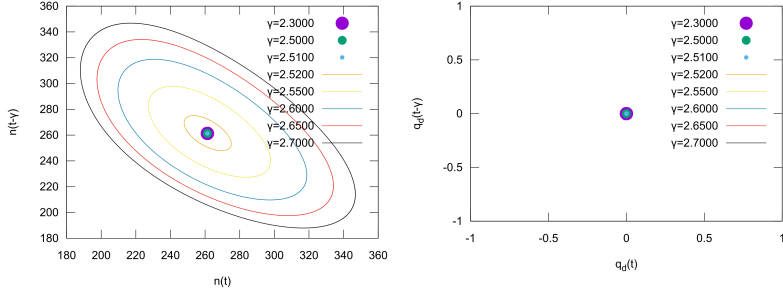


Figure 22: A Hopf bifurcation in n happens for some $\gamma^* \in [2.51, 2.52]$ (region 1 in Fig .21). The fixed point for three values of γ are shown as overlapping dots. Then a periodic orbit appears for $\gamma > 2.51$ that grows in amplitude. The corresponding trajectories of n and q are drawn in the same colours.

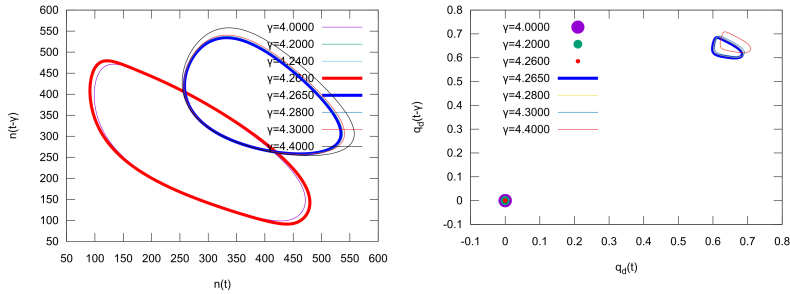


Figure 23: A periodic orbit in q_d appears out of thin air for some $\gamma \in [4.260, 4.265]$ (region 2 in Fig .21). In the right panel we see the red dot that corresponds to a constant value trajectory of q_d for $\gamma = 4.260$ that corresponds to a periodic orbit in n shown as a thick red line on the left. The thick, blue periodic orbit g_d for $\gamma = 4.265$ in the right panel corresponds to the thick, blue orbit for n on the left. The corresponding trajectories of n and q are drawn in the same colours.

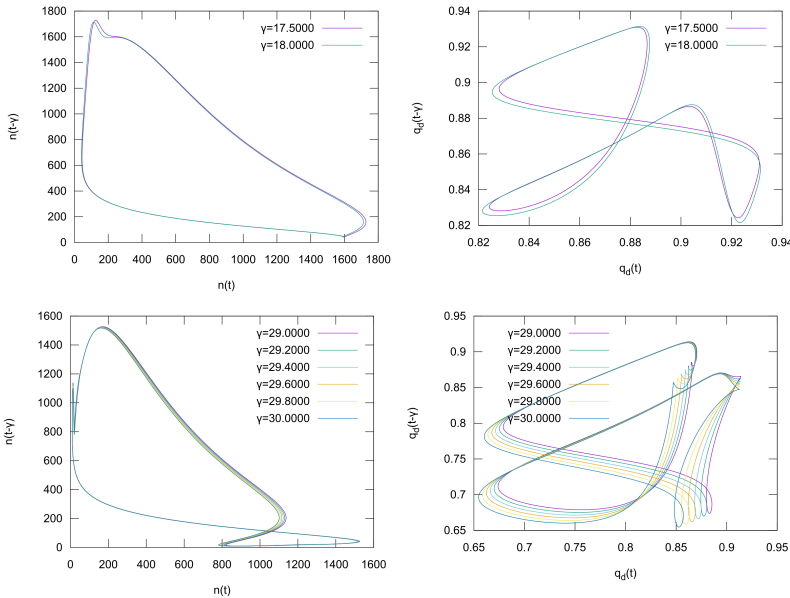


Figure 24: First *kink* in n appears (top panels, region 3 in Fig .21) and then another one in q_d (bottom panels, region 5 in Fig .21). The small kink in n can be seen in the right-bottom corner of the first top panel, while the kink in q_d is larger, and can be seen in the top-right corner of the solution in bottom-right panel. The corresponding trajectories of n and q are drawn in the same colours.

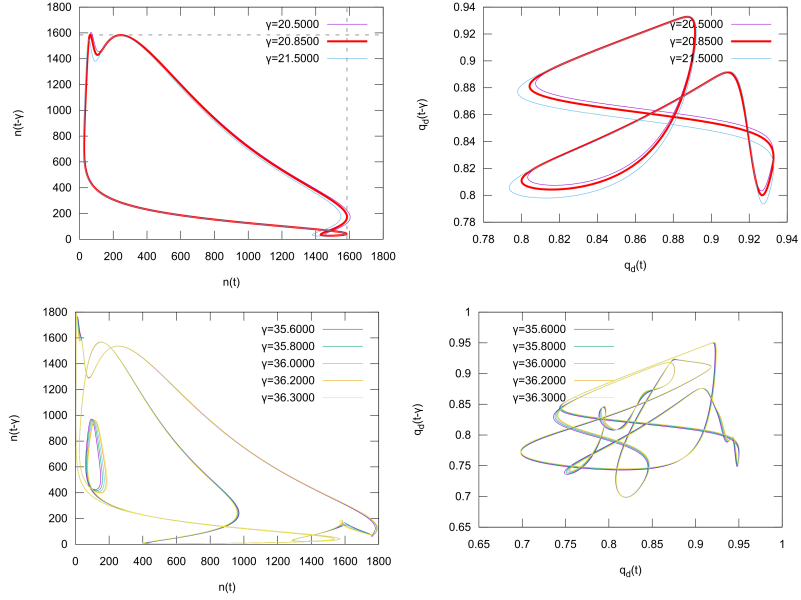


Figure 25: The crossing and folds in periodic orbits (regions 4 and 7 in Fig .21). There is no apparent change in the dynamics and those are kind of artefacts that are caused by using the extrema bifurcation diagrams. The corresponding trajectories of n and q are drawn in the same colours.

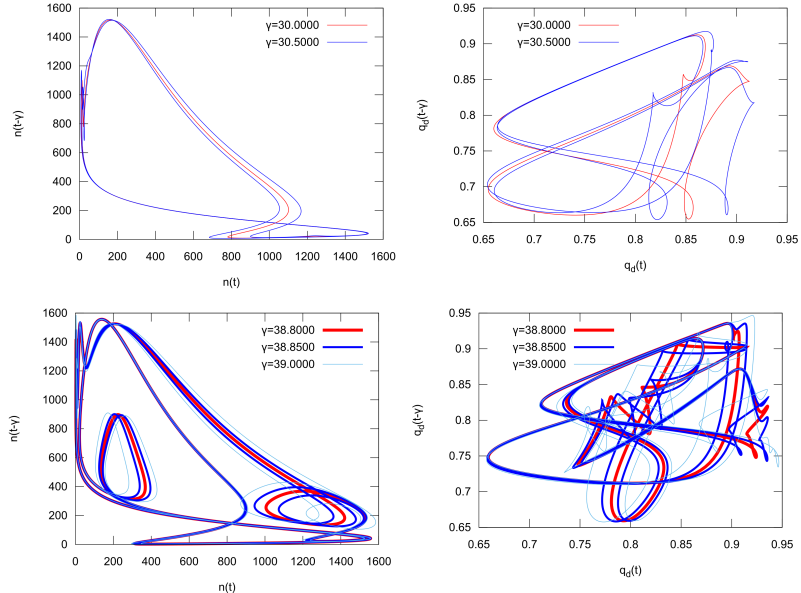


Figure 26: Some examples of a period doubling bifurcation (region 6 and 8 in Fig .21). The trajectory before the period doubling is drawn in red, while the trajectory after the bifurcation is drawn in blue. The corresponding trajectories of n and q are drawn in the same colours.

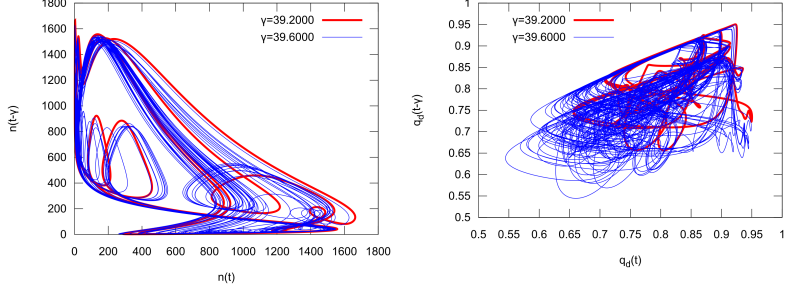


Figure 27: The onset of chaos (region 9 in Fig .21). The trajectory prior to entering the chaotic regime is shown in red. It appears complex, but still resembles a closed curve. The chaotic attractor, shown in blue, is similar to known DDE attractors from the literature. The corresponding trajectories of n and q are drawn in the same colours.

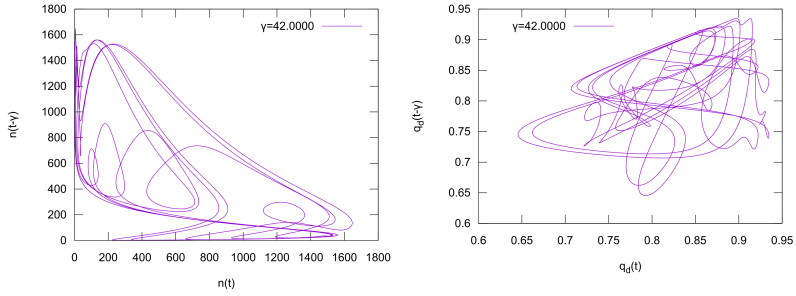


Figure 28: A periodic window (region 10 in Fig .21). The orbit, while complicated, looks like a closed curve. The corresponding trajectories of n and q are drawn in the same colours.

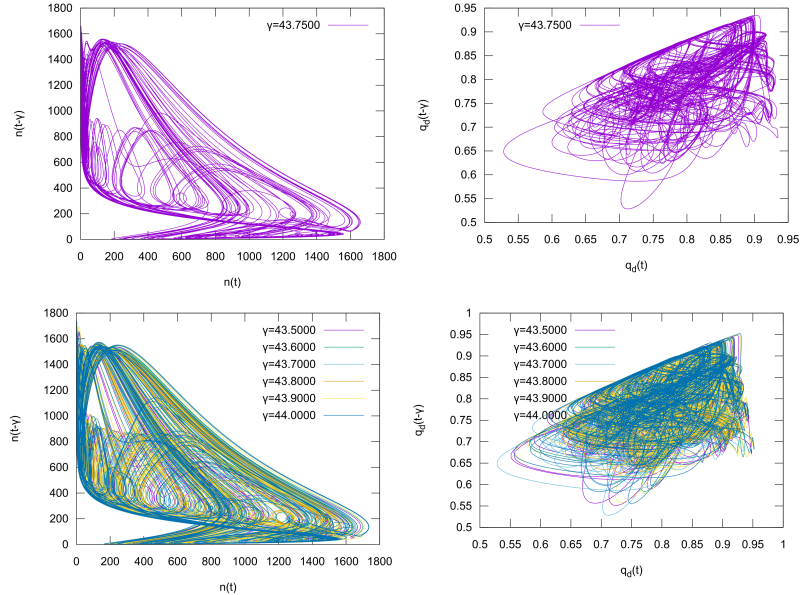


Figure 29: A chaotic attractor (region 11 in Fig .21). In the top panels we have an apparent chaotic attractor for one value of parameter γ , while in the bottom panels we see the superposition of attractors for a range of parameters. It seems that the attractor is changing its shape significantly on this short interval of the parameter. The corresponding trajectories of n and q are drawn in the same colours.

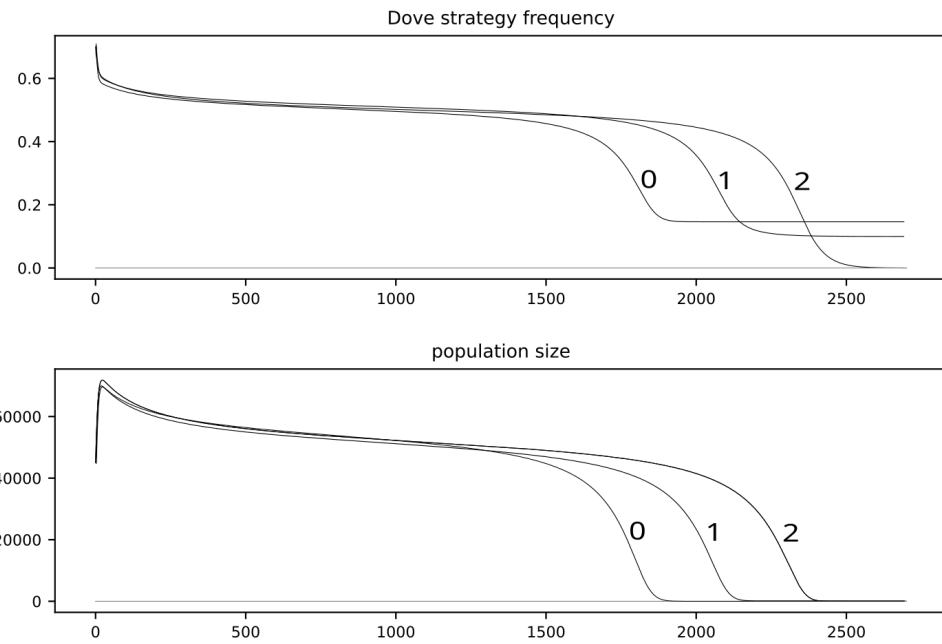


Figure 30: Trajectories of the model generating the ghost attractor and a long transient behavior (parameters: $F = 0.85$, $d = 1$, $\Phi = 0$ and $\Psi = 0.1253$). Trajectories are generated for the undelayed system ($\gamma = 0$), and two cases with short delays ($\gamma = 1$ and $\gamma = 2$). We observe that the classical rest point $q_d = 0.15$, $n = 0$ resulting from the intersection of the frequency nullcline with the trivial density nullcline $n = 0$ loses stability and shifts towards $q_d = 0$ with the increase of the delay. In addition we observe the significant increase of the duration of the long transient phase.

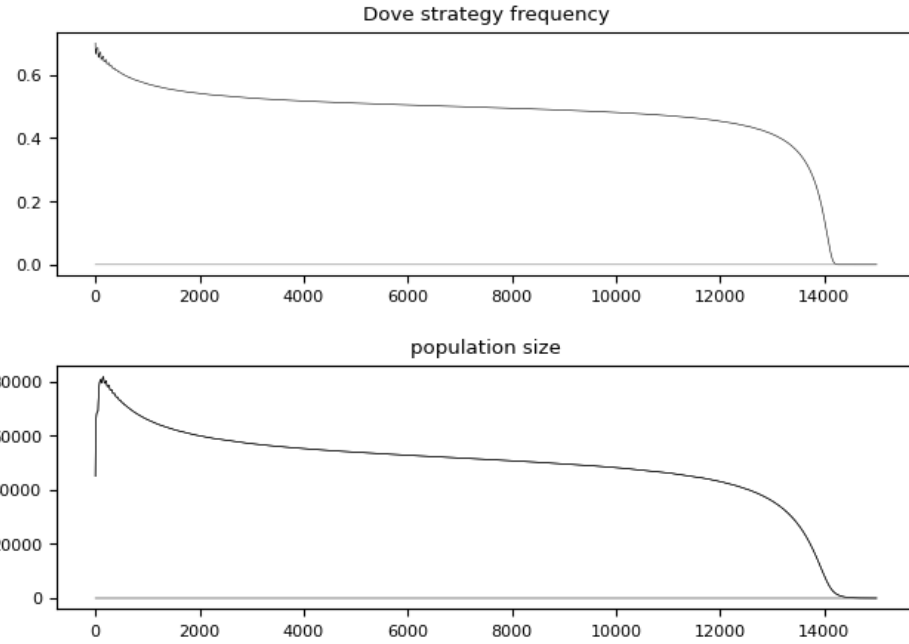


Figure 31: The example with the same parameters as in the Figure 30, but with very long delay $\gamma = 50$. We observe that the duration of the long transient dramatically increased. Thus delays stabilize the ghost attractors.

5 Discussion

In this paper we introduced the delays resulting from maturation time of the juveniles into the eco-evolutionary demographic replicator dynamics [9, 10, 11]. It was shown that the dynamics with delayed fertility rewards produces complex trajectories and is very sensitive to the external factors, even in the simplest case without juvenile recruitment mortality. In general we tested three types of juvenile recruitment: neutral recruitment (juvenile survival equals 1 and the growth is regulated by mortality of adult individuals) and two types of density dependent juvenile survival functions: classical logistic term depending on carrying capacity (interpreted as maximal population load) and suppression term with delay, which should be rather interpreted as the fraction of produced eggs (while fertility payoff describes the maximal potential reproductive output). In addition the model was tested for the response of seasonal mortality, explicit predator pressure (modelled by simple Lotka-Volterra system) and combination of both factors. The resulting trajectories, instead of gradual convergence to the equilibria, as in the classical models, show complicated oscillations before reaching the restpoint. Then the system, similarly to the classical ODE models gradually converges to the stable equilibrium, in area limited by the nullclines. The most extreme phenomena are observed with juvenile survival with the delay. Then we can observe extreme fluctuations, mostly in the population size which can literally oscillate between 3 and 11000. We can observe oscillations in the strategy frequencies too. When we add seasonal mortality those frequency oscillations can take the most extreme form, running from nearly 0 to nearly 1, which is quite unusual for the Hawk-Dove game. In addition, combination of the juvenile suppression with delay and the long maturation time can overturn the strictly game theoretic predictions and prevent the extinction of Doves. Then we observe the extremely complex cyclic or even chaotic dynamics.

Maturation time is very important life-history parameter and the results from this paper show that aspects related to life history theory [32, 31], which is based on demography [19, 20], can seriously affect the trajectories of population dynamics. Therefore, the investigations of the relationships between those fields should be crucial. In the future research we can relax the assumption of uniform delays. Different behavioural types may need different phenotypes, which may need different maturation sizes due to for example different body sizes. In the next step, more detailed models with explicit age or stage structure [29, 28] can be used for confirmation of the predictions obtained in this paper. This can be important from the point of view of the newly emerging eco-evolutionary synthesis [3, 4, 5, 6, 7].

References

- [1] G. E Hutchinson, The ecological theater and the evolutionary play (Yale University Press, 1965).
- [2] Govaert, L., Fronhofer, E. A., Lion, S., Eizaguirre, C., Bonte, D., Egas, M., ... & Matthews, B. (2019). Eco-evolutionary feedbacks—Theoretical models and perspectives. *Functional Ecology*, 33(1), 13-30.
- [3] Post D. M., Palkovacs E. P. (2009). Eco-evolutionary feedbacks in community and ecosystem ecology: interactions between the ecological theatre and the evolutionary play. *Philosophical Transactions of the Royal Society B: Biological Sciences*, 364(1523), 1629-1640.
- [4] Pelletier F., Garant D., Hendry A. P. (2009). Eco-evolutionary dynamics. *Philosophical Transactions of the Royal Society B: Biological Sciences*, 364(1523), 1483-1489.
- [5] Hanski, I. (2012). Eco-evolutionary dynamics in a changing world. *Annals of the New York Academy of Sciences*, 1249(1), 1-17.
- [6] Hendry, A. P. (2017). Eco-evolutionary dynamics. Princeton university press.
- [7] Hendry, A. P. (2019). A critique for eco-evolutionary dynamics. *Functional Ecology*, 33(1), 84-94.
- [8] Pelletier, F., Garant, D., and Hendry, A. P. (2009). Eco-evolutionary dynamics. *Philosophical Transactions of the Royal Society B: Biological Sciences*, 364(1523), 1483-1489.
- [9] K. Argasinski and M. Broom, Ecological theatre and the evolutionary game: how environmental and demographic factors determine payoffs in evolutionary games. *Journal of Mathematical Biology* 67, 935-962 (2013).
- [10] K. Argasinski and M. Broom, Interaction rates, vital rates, background fitness and replicator dynamics: how to embed evolutionary game structure into realistic population dynamics, *Theory in Biosciences* 137, 33-50. (2018).
- [11] K. Argasinski and M. Broom, Evolutionary stability under limited population growth: Eco-evolutionary feedbacks and replicator dynamics. *Ecological Complexity* 34, 198-212 (2018).
- [12] J. Maynard Smith and G. R. Price, The logic of animal conflict, *Nature (London)* 246, 15 (1973).
- [13] J. Maynard Smith, Evolution and the Theory of Games (Cambridge University Press, Cambridge, 1982).
- [14] J. Weibull, Evolutionary Game Theory (MIT Press, Cambridge, MA, 1995).
- [15] J. Hofbauer and K. Sigmund, Evolutionary Games and Population Dynamics (Cambridge University Press, Cambridge, 1998).
- [16] Broom, M., & Rychtář, J. (2022). Game-theoretical models in biology. CRC Press.
- [17] Friedman, D, Sinervo, B (2016). Evolutionary games in natural, social, and virtual worlds. Oxford University Press.
- [18] M Doebeli, Y. Ispolatov, and B. Simon, Towards a mechanistic foundation of evolutionary theory, *Elife* 6, e23804 (2017).
- [19] Metcalf, C. J. E., & Pavard, S. (2007a). Why evolutionary biologists should be demographers. *Trends in Ecology & Evolution*, 22(4), 205-212.
- [20] Metcalf, C. J. E., & Pavard, S. (2007b). All paths to fitness lead through demography. *Trends in Ecology & Evolution*, 22(11), 563-564.
- [21] Bertram, J., & Masel, J. (2019). Density-dependent selection and the limits of relative fitness. *Theoretical population biology*, 129, 81-92.
- [22] Peters, R. H. (1976). Tautology in evolution and ecology. *The American Naturalist*, 110(971), 1-12.
- [23] Peters, R. H. (1978). Predictable problems with tautology in evolution and ecology. *The American Naturalist*, 112(986), 759-762.

[24] , Van Der Steen W. J. (1983). Methodological problems in evolutionary biology I. Testability and tautologies. *Acta biotheoretica*, 32(3), 207-215.

[25] von Sydow, M. (2016). 'Survival of the Fittest' in Darwinian Metaphysics: Tautology or Testable Theory?. In *Reflecting on Darwin* (pp. 199-222). Routledge.

[26] Argasinski K. Rudnicki R. (2017). Nest site lottery revisited: Towards a mechanistic model of population growth suppressed by the availability of nest sites. *Journal of Theoretical Biology*, 420, 279-289.

[27] Argasinski K. Rudnicki R. (2020). From nest site lottery to host lottery: continuous model of growth suppression driven by the availability of nest sites for newborns or hosts for parasites and its impact on the selection of life history strategies. *Theory in Biosciences*, 139(2), 171-188.

[28] Argasinski K. Rudnicki R. (2021). Replicator dynamics for the game theoretic selection models based on state. *Journal of Theoretical Biology*, 526, 110540.

[29] Argasinski K. Broom M. (2021). Towards a replicator dynamics model of age structured populations. *Journal of Mathematical Biology*, 82, 1-39.

[30] Houston, A. I., & McNamara, J. M. (1999). Models of adaptive behaviour: an approach based on state. Cambridge University Press.

[31] Roff, D. (Ed.). (1993). *Evolution of life histories: theory and analysis*. Springer Science & Business Media.

[32] Stearns, S. C. (1992). *The evolution of life histories* (Vol. 249, p. xii). Oxford: Oxford university press.

[33] Railsback, S. F. and Grimm, V. (2019). *Agent-based and individual-based modeling: a practical introduction*. Princeton university press.

[34] Araujo, G. (2025). An evolutionary game theory for event-driven ecological population dynamics. *Theory in Biosciences*, 144(1), 95-105.

[35] Alboszta, J., & Miękisz, J. (2004). Stability of evolutionarily stable strategies in discrete replicator dynamics with time delay. *Journal of theoretical biology*, 231(2), 175-179.

[36] Ben-Khalifa, N., El-Azouzi, R., & Hayel, Y. (2018). Discrete and continuous distributed delays in replicator dynamics. *Dynamic Games and Applications*, 8, 713-732.

[37] Zhong, C. Yang, H. Liu, Z. Wu J. (2020). Stability of replicator dynamics with bounded continuously distributed time delay. *Mathematics*, 8(3), 431.

[38] Zhong C. Wang N. Yang H. Zhao W. (2021). Robust Stability of Uncertain Replicator Population Dynamics with Time Delay. In *Simulation Tools and Techniques: 12th EAI International Conference, SIMUtools 2020, Guiyang, China, August 28-29, 2020, Proceedings, Part II 12* (pp. 15-28). Springer International Publishing.

[39] Miękisz J, Bodnar M. Evolution of populations with strategy-dependent time delays. *Physical Review E*. 2021 Jan 22;103(1):012414.

[40] Mohamadichamgavi J, Bodnar M. (2025). Bifurcation Analysis of Replicator Dynamics with Logistic Growth and Strategy-Dependent Time Delays in Snowdrift Game. *Dynamic Games and Applications*, 1-29.

[41] McNamara, J. M. (2013). Towards a richer evolutionary game theory. *Journal of the Royal Society Interface*, 10(88), 20130544.

[42] C. Hui, Carrying capacity, population equilibrium, and environment's maximal load, *Ecological Modelling* 192, 317-320 (2006).

[43] Holling, C. S. (1973). Resilience and stability of ecological systems, *Annual Review of Ecology and Systematics*, Vol. 4, 1-23 (1973)

[44] Holling, C. S. (1996). Engineering resilience versus ecological resilience, *Engineering within ecological constraints*, ed. Peter Schultze 32. 31-43 (1996).

[45] Meyer, K. (2016). A mathematical review of resilience in ecology. *Natural Resource Modeling* 29(3), 339-352.

[46] Krakovska, H., Kuehn, C., & Longo, I. P. (2024). Resilience of dynamical systems. *European Journal of Applied Mathematics*, 35(1), 155-200.

[47] Reed, J. M., Wolfe, B. E., & Romero, L. M. (2024). Is resilience a unifying concept for the biological sciences?. *IScience* 27, 5, 109478

[48] Lakshmikantham V, Bainov D, Simeonov P (1989) Theory of Impulsive Differential Equations. World Scientific, Singapore

[49] Sahoo, D., and Samanta, G. (2023). Modeling cooperative evolution in prey species using the snowdrift game with evolutionary impact on prey-predator dynamics. *Chaos, Solitons and Fractals*, 177, 114269.

[50] Sabin, G.C. and Summers, D., (1993). Chaos in a periodically forced predator-prey ecosystem model. *Mathematical Biosciences*, 113(1), pp.91-113.

[51] Inoue, M. and Kamifukumoto, H., (1984). Scenarios leading to chaos in a forced Lotka-Volterra model. *Progress of Theoretical Physics*, 71(5), pp.930-937.

[52] Rinaldi, S. and Muratori, S., (1993). Conditioned chaos in seasonally perturbed predator-prey models. *Ecological Modelling*, 69(1-2), pp.79-97.

[53] Tang, S. and Chen, L., (2002). Density-dependent birth rate, birth pulses and their population dynamic consequences. *Journal of Mathematical Biology*, 44(2), pp.185-199.

[54] Liu, Xianning, and Lansun Chen (2003). "Complex dynamics of Holling type II Lotka–Volterra predator–prey system with impulsive perturbations on the predator." *Chaos, Solitons and Fractals* 16, no. 2: 311-320.

[55] Peixoto, M. M. (1959). On structural stability. *Annals of Mathematics*, 69(1), 199-222.

[56] Arnold, V. I. (1983). Geometrical methods in the theory of ordinary differential equations. Springer-Verlag.

[57] Schuster P, Sigmund K, Wolff R (1979) Dynamical systems under constant organization 3: cooperative and competitive behavior of hypercycles. *J Differential Equations* 32:357–368

[58] Sigmund K, Schuster P (1984) Permanence and uninvasability for deterministic population models. In *Stochastic phenomena and chaotic behaviour in complex systems*, pages 173–184. Springer

[59] Schreiber SJ (2000) Criteria for cr robust permanence. *J Differential Equations* 162(2):400–426

[60] Schreiber SJ, Benaïm M, Atchadé KAS (2011) Persistence in fluctuating environments. *J Math Biol* 62:655–683

[61] Hofbauer J, Schreiber SJ (2022) Permanence via invasion graphs: incorporating community assembly into modern coexistence theory. *J Math Biol* 85(5):54

[62] Jansen VAA, Sigmund K (1998) Shaken not stirred: on permanence in ecological communities. *Theor Popul Biol* 54:195–201

[63] Morozov, A., Feudel, U., Hastings, A., Abbott, K.C., Cuddington, K., Heggerud, C.M. and Petrovskii, S., 2024. Long-living transients in ecological models: Recent progress, new challenges, and open questions. *Physics of Life Reviews* 51, 423-441 (2024)

[64] A. Morozov K. Abbott K. Cuddington T. Francis G. Gellner A. Hastings Y.-C. Lai S. Petrovskii K. Scranton and M. L. Zeeman Long transients in ecology: Theory and applications, *Physics of Life Reviews* 32, 1 (2020).

[65] A. Hastings, Transients: the key to long-term ecological understanding?, *Trends in Ecology & Evolution* 19, 39 (2004).

[66] A. Hastings, K. C. Abbott, K. Cuddington, T. Francis, G. Gellner, Y.-C. Lai, A. Morozov, S. Petrovskii, K. Scranton, and M. L. Zeeman, Transient phenomena in ecology, *Science* 361, eaat6412 (2018).

[67] Szczelina R., P. Zgliczyński P.. High-order Lohner-type algorithm for rigorous computation of Poincaré maps in systems of delay differential equations with several delays. *Found. Comput. Math.*, 24(4):1389–1454, 2024

[68] Leandro Junges, Gallas J.A.C. Intricate routes to chaos in the mackey–glass delayed feedback system. *Physics Letters A*, 376(30):2109–2116, 2012.

[69] Duruisseau V. Humphries A.R.. Bistability, bifurcations and chaos in the Mackey-Glass equation. *Journal of Computational Dynamics*, 9(3):421–450, 2022.

[70] Szczelina R.. Source codes for generating bifurcation diagrams. <https://github.com/robsontpm/ddes-evo-game>. Accessed: 2025-07-25.

[71] Anna Gierzkiewicz, Robert Szczelina. Sharkovskii theorem for infinite dimensional dynamical systems. *Communications in Nonlinear Science and Numerical Simulation*, 146:108770, 2025.

[72] Gábor Benedek G., Krisztin T., Szczelina R.. Stable periodic orbits for delay differential equations with unimodal feedback. *Journal of Dynamics and Differential Equations*, 2024. To appear; published online 2024-12-10

[73] Ansmann, G. (2018). Efficiently and easily integrating differential equations with JiTCODE, JiTCODE, and JiTCODE. *Chaos: An interdisciplinary journal of nonlinear science*, 28(4).

[74] Koch, D., Nandan, A., Ramesan, G., Tyukin, I., Gorban, A. and Koseska, A., 2024. Ghost channels and ghost cycles guiding long transients in dynamical systems. *Physical Review Letters*, 133(4), p.047202.

[75] Cheng, H., Meng, X., Hayat, T., and Hobiny, A. (2022). Dynamics analysis for a prey-predator evolutionary game system with delays. *Dynamic Games and Applications*, 1-28.

[76] Gerlee, P. (2022). Weak selection and the separation of eco-evo time scales using perturbation analysis. *Bulletin of Mathematical Biology*, 84(5), 52.

[77] Gunderson, L. H., Allen, C. R., & Holling, C. S. (Eds.). (2012). *Foundations of ecological resilience*. Island Press.

[78] Cressman R, Garay J (2003) Stability in n-species coevolutionary systems. *Theor Popul Biol* 64(4):519–533

[79] P. D. Taylor and L. B. Jonker, Evolutionarily stable strategy and game dynamics, *Math. Biosci.* 40, 145 (1978).

[80] J. Hofbauer, P. Shuster, and K. Sigmund, A note on evolutionarily stable strategies and game dynamics, *J. Theor. Biol.* 81, 609 (1979).

[81] <https://github.com/ReplicatorDynamics/Delayed-Replicator-Dynamics>

5.1 Appendix 1

Recall the fertility payoffs are

$$\begin{aligned}
 V_H &= (1 - q_d)0.5F + q_dF = (1 + q_d)0.5F \\
 V_D &= q_d0.5F + (1 - q_d)0 = q_d0.5F \\
 \bar{V} &= (1 - q_d)V_H + q_dV_D = (1 - q_d)(1 + q_d)0.5F + q_d^20.5F \\
 &= [(1 - q_d)(1 + q_d) + q_d^2]0.5F = 0.5F
 \end{aligned}$$

Mortality payoffs are

$$\begin{aligned}
 D_H &= (1 - q_d)0.5d \text{ and } D_D = 0 \\
 \bar{D} &= (1 - q_d)D_H + q_dD_D = (1 - q_d)^20.5d
 \end{aligned}$$

Bracketed terms are $(V_D - \bar{V}) = -(1 - q_d)0.5F$ and $(D_D - \bar{D}) = -(1 - q_d)^20.5d$ leading to the system

$$\frac{dq_d}{dt} = 0.5q_d(t)(1 - q_d(t)) \left((1 - q_d(t))d - \left(1 - \frac{n(t)}{K}\right)F \right) \quad (37)$$

$$\frac{dn}{dt} = n(t) \left((0.5F + \Phi) \left(1 - \frac{n(t)}{K}\right) - \left[(1 - q_d(t))^20.5d + \Psi\right] \right). \quad (38)$$

Calculation of the nullclines: Nullclines are solutions of zeros of the r.h.s. of the equations:

$$(1 - q_d) d - \left(1 - \frac{n}{K}\right) F = 0 \implies q_d = 1 - \left(1 - \frac{n}{K}\right) \frac{F}{d}. \quad (39)$$

Nullcline for the population size will be

$$(0.5F + \Phi) \left(1 - \frac{n}{K}\right) - \left[(1 - q_d)^2 0.5d + \Psi\right] = 0 \quad (40)$$

$$1 - \frac{n}{K} = \frac{(1 - q_d)^2 0.5d + \Psi}{0.5F + \Phi} \quad (41)$$

$$n(t) = \left[1 - \frac{(1 - q_d)^2 0.5d + \Psi}{0.5F + \Phi}\right] K. \quad (42)$$

Calculation of the rest points: The rest points will be intersections of both nullclines.

$$\begin{aligned} q_d &= 1 - \left(\frac{(1 - q_d)^2 0.5d + \Psi}{0.5F + \Phi}\right) \frac{F}{d} \\ q_d &= 1 - \frac{(1 - q_d)^2 0.5 + \frac{\Psi}{d}}{\left(0.5 + \frac{\Phi}{F}\right)} \\ (1 - q_d) \left(0.5 + \frac{\Phi}{F}\right) &= (1 - q_d)^2 0.5 + \frac{\Psi}{d} \\ \left(0.5 + \frac{\Phi}{F}\right) - q_d \left(0.5 + \frac{\Phi}{F}\right) &= (1 - q_d)^2 0.5 + \frac{\Psi}{d} \\ \left(0.5 + \frac{\Phi}{F}\right) - q_d \left(0.5 + \frac{\Phi}{F}\right) &= (1 - 2q_d + q_d^2) 0.5 + \frac{\Psi}{d} \\ \left(0.5 + \frac{\Phi}{F}\right) - q_d \left(0.5 + \frac{\Phi}{F}\right) &= 0.5 - q_d + 0.5q_d^2 + \frac{\Psi}{d} \\ 0.5q_d^2 + \left(\frac{\Phi}{F} - 0.5\right) q_d - \frac{\Phi}{F} + \frac{\Psi}{d} &= 0 \end{aligned}$$

Let us solve this equation. The Δ will provide the condition of existence of the nullcline intersections

$$\begin{aligned} \Delta &= \left(\frac{\Phi}{F} - 0.5\right)^2 - 2\left(\frac{\Psi}{d} - \frac{\Phi}{F}\right) = \frac{\Phi^2}{F} - \frac{\Phi}{F} + 0.25 - 2\frac{\Psi}{d} + 2\frac{\Phi}{F} = \frac{\Phi^2}{F} + \frac{\Phi}{F} - 2\frac{\Psi}{d} + 0.25 \\ &= \left(\frac{\Phi}{F} + 0.5\right)^2 - 2\frac{\Psi}{d}, \end{aligned}$$

Then for $\Delta > 0$ we have two rest point frequencies:

$$\begin{aligned} \check{q}_d &= 0.5 - \frac{\Phi}{F} - \sqrt{\left(\frac{\Phi}{F}\right)^2 + \frac{\Phi}{F} - 2\frac{\Psi}{d} + 0.25} \\ \hat{q}_d &= 0.5 - \frac{\Phi}{F} + \sqrt{\left(\frac{\Phi}{F}\right)^2 + \frac{\Phi}{F} - 2\frac{\Psi}{d} + 0.25} \end{aligned}$$

Let's now substitute those values into the density nullcline and calculate the respective population sizes

$$\begin{aligned}
(1 - q_d)^2 &= \left(0.5 + \frac{\Phi}{f} \pm \sqrt{\Delta}\right)^2 \\
&= \left(0.5 + \frac{\Phi}{f}\right)^2 \pm \left(1 + 2\frac{\Phi}{f}\right) \sqrt{\Delta} + \Delta \\
&= \left(0.5 + \frac{\Phi}{f}\right)^2 \pm \left(1 + 2\frac{\Phi}{f}\right) \sqrt{\Delta} + \left(\frac{\Phi}{f} + 0.5\right)^2 - 2\frac{\Psi}{d} \\
&= 2\left(0.5 + \frac{\Phi}{f}\right)^2 \pm \left(1 + 2\frac{\Phi}{f}\right) \sqrt{\Delta} - 2\frac{\Psi}{d} \\
&= 2 \left[\left(0.5 + \frac{\Phi}{f}\right)^2 \pm \left(0.5 + \frac{\Phi}{f}\right) \sqrt{\Delta} - \frac{\Psi}{d} \right]
\end{aligned}$$

then the juvenile survival term is

$$\begin{aligned}
\mathbf{D}(n) &= \frac{(1 - q_d)^2 0.5d + \Psi}{0.5f + \Phi} \\
&= \frac{d (1 - q_d)^2 0.5 + \frac{\Psi}{d}}{f \left(0.5 + \frac{\Phi}{f}\right)} \\
&= \frac{d \left(0.5 + \frac{\Phi}{f}\right)^2 \pm \left(0.5 + \frac{\Phi}{f}\right) \sqrt{\Delta}}{f \left(0.5 + \frac{\Phi}{f}\right)} \\
&= \frac{d}{f} \left(0.5 + \frac{\Phi}{f}\right) \pm \sqrt{\Delta}
\end{aligned}$$

For the logistic suppression $\mathbf{D}(n) = (1 - \frac{n}{K})$ the density in the rest points will be

$$n = \left[1 - \frac{d}{f} \left(0.5 + \frac{\Phi}{f}\right) \mp \sqrt{\Delta}\right] K$$

Now we can infer the stability of the rest points. According to the Lemma 2 in [11] when the derivative with respect to n of the r.h.s. of the frequency equation (11) is positive (in our case it equals to $0.5q_d(1 - q_d)F/K > 0$), then the slopes along the q_d axis of the frequency (S_q) and density (S_n) nullclines should satisfy condition $S_n < S_q$. Nullcline derivatives are $\frac{dq_d(n)}{dn} = \frac{F}{dK}$ (then the slope along q_d axis is $S_q = \frac{dK}{F}$) and $S_n = \frac{d\tilde{n}(q_d)}{dq_d} = \frac{(1 - q_d)}{0.5F + \Phi} dK$. Then the condition $S_n < S_q$ is

$$\frac{(1 - q_d)}{0.5F + \Phi} dK < \frac{dK}{F} \implies (1 - q_d) < 0.5 + \frac{\Phi}{F} \implies q_d > 0.5 - \frac{\Phi}{F}.$$

Therefore, intersection $q_d < 0.5 - \frac{\Phi}{F}$ is a saddle point while intersection $q_d > 0.5 - \frac{\Phi}{F}$ is stable attractor. The condition on nullcline slopes is clearly visible on numerical solutions.

5.2 Appendix 2

Per capita fertility rate is

$$\begin{aligned} \frac{n_1(t-\gamma)}{n_1(t)} e_1 V q^T(t-\gamma) &= \frac{n(t-\gamma) \frac{n_1(t-\gamma)}{n(t)}}{n(t) \frac{n_1(t)}{n(t)}} e_1 V q^T(t-\gamma) \\ &= \frac{n(t-\gamma) q_1(t-\gamma)}{n(t) q_1(t)} e_1 V q^T(t-\gamma). \end{aligned}$$

the average fertility rate is

$$\sum_i q_i(t) \frac{n(t-\gamma) q_i(t-\gamma)}{n(t) q_i(t)} e_i V q^T(t-\gamma) = \frac{n(t-\gamma)}{n(t)} \sum_i q_i(t-\gamma) e_i V q^T(t-\gamma)$$

In effect the fertility bracketed term will be

$$\begin{aligned} & q_1(t) \left[\frac{n(t-\gamma) q_1(t-\gamma)}{n(t) q_1(t)} e_1 V q^T(t-\gamma) - \frac{n(t-\gamma)}{n(t)} \sum_i q_i(t-\gamma) e_i V q^T(t-\gamma) \right] \\ &= \frac{n(t-\gamma)}{n(t)} \left[q_1(t-\gamma) e_1 V q^T(t-\gamma) - q_1(t) \sum_i q_i(t-\gamma) e_i V q^T(t-\gamma) \right] \end{aligned}$$

Note that the above dynamics is well defined and cannot escape the unit interval. For $q_1(t) = 0$ fertility bracket equals $q_1(t-\gamma) V_1(t-\gamma) \geq 0$ while for $q_1(t) = 1$ it is $[q_1(t-\gamma) V_1(t-\gamma) - \bar{V}(t-\gamma)]$

$$\begin{aligned} & [q_1(t-\gamma) V_1(t-\gamma) - \bar{V}(t-\gamma)] \\ &= q_1(t-\gamma) V_1(t-\gamma) - q_1(t-\gamma) V_1(t-\gamma) - \sum_{i \neq 1} q_i(t-\gamma) V_i(t-\gamma) \\ &= - \sum_{i \neq 1} q_i(t-\gamma) V_i(t-\gamma) \leq 0 \end{aligned}$$

For two competing strategies the fertility bracketed term reduces to

$$\begin{aligned} & q_1(t-\gamma) V_1(t-\gamma) - q_1(t) \bar{V}(t-\gamma) \\ &= q_1(t-\gamma) V_1(t-\gamma) - q_1(t) [q_1(t-\gamma) V_1(t-\gamma) + (1 - q_1(t-\gamma)) V_2(t-\gamma)] \\ &= q_1(t-\gamma) V_1(t-\gamma) - q_1(t) q_1(t-\gamma) V_1(t-\gamma) - q_1(t) (1 - q_1(t-\gamma)) V_2(t-\gamma) \\ &= [1 - q_1(t)] q_1(t-\gamma) V_1(t-\gamma) - q_1(t) (1 - q_1(t-\gamma)) V_2(t-\gamma) \end{aligned}$$

5.3 Appendix 3

Proof. Recall that the point (n^*, n_1^*) is a stable point for the system without delay ($\gamma = 0$). Now we looking for $\gamma > 0$ when the system (17)–(18) loses its stability. The linearized system is of the form

$$\mathbf{x}'(t) = b_{11} \mathbf{x}(t) + b_{12} \mathbf{x}(t-\gamma) + b_{13} \mathbf{y}(t) + b_{14} \mathbf{y}(t-\gamma), \quad (43)$$

$$\mathbf{y}'(t) = b_{21} \mathbf{x}(t) + b_{22} \mathbf{x}(t-\gamma) + b_{23} \mathbf{y}(t) + b_{24} \mathbf{y}(t-\gamma). \quad (44)$$

Next we substitute to this system $\mathbf{x}(t) = e^{cti}$ and $\mathbf{y}(t) = \beta e^{cti}$ and obtain a system of algebraic equations for c , β and γ :

$$ci = b_{11} + b_{12} e^{-c\gamma i} + b_{13} \beta + b_{14} \beta e^{-c\gamma i}, \quad (45)$$

$$\beta ci = b_{21} + b_{22} e^{-c\gamma i} + b_{23} \beta + b_{24} \beta e^{-c\gamma i}. \quad (46)$$

The bifurcation point, is the minimum value of γ for which there is a real number c and a complex number β satisfying system (45)–(46). Deriving β from equations (45)–(46), we get

$$\frac{-ci + b_{11} + b_{12} e^{-c\gamma i}}{b_{13} + b_{14} e^{-c\gamma i}} = \frac{b_{21} + b_{22} e^{-c\gamma i}}{-ci + b_{23} + b_{24} e^{-c\gamma i}}. \quad (47)$$

Let $z = e^{-c\gamma i}$. Then we have

$$\frac{-ci + b_{11} + b_{12}z}{b_{13} + b_{14}z} = \frac{b_{21} + b_{22}z}{-ci + b_{23} + b_{24}z}, \quad (48)$$

$$(b_{11} + b_{12}z - ci)(b_{23} + b_{24}z - ci) = (b_{21} + b_{22}z)(b_{13} + b_{14}z) \quad (49)$$

$$b_{12}b_{24}z^2 + (b_{11}b_{24} + b_{23}b_{12})z - (b_{12} + b_{24})ci - (b_{23} + b_{11})ci + b_{11}b_{23} - c^2 = \quad (50)$$

$$b_{22}b_{14}z^2 + (b_{14}b_{21} + b_{22}b_{13})z + b_{21}b_{13} \quad (51)$$

This leads to the quadratic equation on z

$$(b_{12}b_{24} - b_{22}b_{14})z^2 + (b_{11}b_{24} + b_{23}b_{12} - b_{14}b_{21} - b_{22}b_{13} - (b_{12} + b_{24})ci)z + b_{11}b_{23} - b_{21}b_{13} - (b_{23} + b_{11})ci - c^2 = 0,$$

which can be presented in the form:

$$Az^2 + \tilde{B}z + \tilde{C} = 0, \quad (52)$$

where

$$A = b_{12}b_{24} - b_{22}b_{14},$$

$$\tilde{B} = b_{11}b_{24} + b_{12}b_{23} - b_{14}b_{21} - b_{22}b_{13} - (b_{12} + b_{24})ci,$$

$$\tilde{C} = b_{11}b_{23} - b_{21}b_{13} - (b_{11} + b_{23})ci - c^2$$

Then z is the solution of the above equation. Since $z\bar{z} = 1$, we obtain from Eq. (52) that

$$Az + \tilde{B} + \tilde{C}\bar{z} = 0. \quad (53)$$

Let $z = X + Yi$, where X, Y are real numbers. Since $\text{Im}(\tilde{B}) = -(b_{12} + b_{24})c$ and $\text{Im}(\tilde{C}) = -(b_{11} + b_{23})c$ we have

$$Az = AX + AYi \quad \text{and} \quad \tilde{C}\bar{z} = \Re(\tilde{C})X + \text{Im}(\tilde{C})Y + (\text{Im}(\tilde{C})X - \Re(\tilde{C})Y)i$$

from Eq. (53) we obtain

$$(A + \Re(\tilde{C}))X + \text{Im}(\tilde{C})Y = -\Re(\tilde{B}), \quad (54)$$

$$\text{Im}(\tilde{C})X + (A - \Re(\tilde{C}))Y = -\text{Im}(\tilde{B}), \quad (55)$$

The parts independent of c of A , \tilde{B} and \tilde{C} are:

$$A = b_{12}b_{24} - b_{22}b_{14},$$

$$B = b_{11}b_{24} + b_{12}b_{23} - b_{13}b_{22} - b_{14}b_{21},$$

$$C = b_{11}b_{23} - b_{13}b_{21},$$

thus $\Re(\tilde{B}) = B$ and $\Re(\tilde{C}) = C - c^2$. Then system (54,55) is

$$(A + [C - c^2])X - (b_{11} + b_{23})cY = -B,$$

$$-(b_{11} + b_{23})cX + (A - [C - c^2])Y = (b_{12} + b_{24})c,$$

then from the Cramer formulae we obtain:

$$W = \begin{vmatrix} A + [C - c^2] & -(b_{11} + b_{23})c \\ -(b_{11} + b_{23})c & A - [C - c^2] \end{vmatrix} = A^2 - [C - c^2]^2 - (b_{11} + b_{23})^2c^2$$

$$W_X = \begin{vmatrix} -B & -(b_{11} + b_{23})c \\ (b_{12} + b_{24})c & A - [C - c^2] \end{vmatrix} = -B(A - [C - c^2]) + (b_{11} + b_{23})(b_{12} + b_{24})c^2$$

$$W_Y = \begin{vmatrix} (A + \Re(C)) & -\Re(B) \\ -(b_{11} + b_{23})c & (b_{12} + b_{24})c \end{vmatrix} = (A + [C - c^2])(b_{12} + b_{24})c - B(b_{11} + b_{23})c$$

then

$$X = \frac{W_X}{W} = \frac{-B(A - [C - c^2]) + (b_{11} + b_{23})(b_{12} + b_{24})c^2}{A^2 - [C - c^2]^2 - (b_{11} + b_{23})^2c^2},$$

$$Y = \frac{W_Y}{W} = \frac{(A + [C - c^2])(b_{12} + b_{24})c - B(b_{11} + b_{23})c}{A^2 - [C - c^2]^2 - (b_{11} + b_{23})^2c^2}.$$

Then from Euler's formula we have $z = e^{-c\gamma i} = \cos(-c\gamma) + i \sin(-c\gamma)$, thus $X^2 + Y^2 = 1$. This leads to the equation:

$$\begin{aligned} & [-B(A - C + c^2) + (b_{11} + b_{23})(b_{12} + b_{24})c^2]^2 \\ & + [(A + C - c^2)(b_{12} + b_{24})c - B(b_{11} + b_{23})c]^2 \\ & = [(b_{11} + b_{23})^2c^2 + ([C - c^2]^2 - A^2)]^2. \end{aligned}$$

then we can expand the respective parts of the above equation. First bracketed term on the left hand side is:

$$\begin{aligned} & [(b_{11} + b_{23})(b_{12} + b_{24})c^2 - B(A - C + c^2)]^2 \\ & = [(b_{11} + b_{23})(b_{12} + b_{24})]^2 c^4 \\ & \quad - 2(b_{11} + b_{23})(b_{12} + b_{24})c^2 B(A - C + c^2) \\ & \quad + B^2(A - C + c^2)^2 \\ & = [(b_{11} + b_{23})(b_{12} + b_{24})]^2 c^4 \\ & \quad - 2(b_{11} + b_{23})(b_{12} + b_{24})(A - C)Bc^2 \\ & \quad - 2(b_{11} + b_{23})(b_{12} + b_{24})Bc^4 \\ & \quad + B^2(A - C)^2 + 2B^2(A - C)c^2 + B^2c^4 \\ & = \left([(b_{11} + b_{23})(b_{12} + b_{24})]^2 - 2(b_{11} + b_{23})(b_{12} + b_{24})B + B^2 \right) c^4 \\ & \quad + (2B^2(A - C) - 2(b_{11} + b_{23})(b_{12} + b_{24})(A - C)B)c^2 \\ & \quad + B^2(A - C)^2 \\ & = ((b_{11} + b_{23})(b_{12} + b_{24}) - B)^2 c^4 \\ & \quad + 2B(A - C)(B - (b_{11} + b_{23})(b_{12} + b_{24}))c^2 \\ & \quad + B^2(A - C)^2 \end{aligned}$$

second bracketed term on the left hand side is

$$\begin{aligned}
& [(A + C - c^2)(b_{12} + b_{24})c - B(b_{11} + b_{23})c]^2 \\
&= c^2 [(A + C - c^2)^2(b_{12} + b_{24})^2 - 2(A + C - c^2)(b_{12} + b_{24})(b_{11} + b_{23})B + (b_{11} + b_{23})^2B^2] \\
&= c^2 [(A + C)^2 - 2(A + C)c^2 + c^4)(b_{12} + b_{24})^2 \\
&\quad - 2(A + C)(b_{12} + b_{24})(b_{11} + b_{23})B + 2(b_{12} + b_{24})(b_{11} + b_{23})Bc^2 \\
&\quad + (b_{11} + b_{23})^2B^2] \\
&= c^2 [(A + C)^2(b_{12} + b_{24})^2 - 2(A + C)(b_{12} + b_{24})^2c^2 + (b_{12} + b_{24})^2c^4 \\
&\quad + 2(b_{12} + b_{24})(b_{11} + b_{23})Bc^2 \\
&\quad + (b_{11} + b_{23})^2B^2 - 2(A + C)(b_{12} + b_{24})(b_{11} + b_{23})B] \\
&= c^2 [(b_{12} + b_{24})^2c^4 \\
&\quad + [2(b_{12} + b_{24})(b_{11} + b_{23})B - 2(A + C)(b_{12} + b_{24})^2]c^2 \\
&\quad + (A + C)^2(b_{12} + b_{24})^2 - 2(A + C)(b_{12} + b_{24})(b_{11} + b_{23})B + (b_{11} + b_{23})^2B^2] \\
&= c^2 [(b_{12} + b_{24})^2c^4 \\
&\quad + [2(b_{12} + b_{24})(b_{11} + b_{23})B - 2(A + C)(b_{12} + b_{24})^2]c^2 \\
&\quad + ((A + C)(b_{12} + b_{24}) - (b_{11} + b_{23})B)^2] \\
&= (b_{12} + b_{24})^2c^6 \\
&\quad + [2(b_{12} + b_{24})(b_{11} + b_{23})B - 2(A + C)(b_{12} + b_{24})^2]c^4 \\
&\quad + ((A + C)(b_{12} + b_{24}) - (b_{11} + b_{23})B)^2c^2
\end{aligned}$$

third bracketed term located on the right hand side is

$$\begin{aligned}
& [(b_{11} + b_{23})^2c^2 + (C - c^2)^2 - A^2]^2 \\
&= [(b_{11} + b_{23})^2c^2 + C^2 - 2Cc^2 + c^4 - A^2]^2 \\
&= [c^4 + ((b_{11} + b_{23})^2 - 2C)c^2 + C^2 - A^2]^2 \\
&= (c^2 + ((b_{11} + b_{23})^2 - 2C))^2c^4 \\
&\quad + 2(c^4 + ((b_{11} + b_{23})^2 - 2C)c^2)(C^2 - A^2) \\
&\quad + (C^2 - A^2)^2 \\
&= (c^4 + 2((b_{11} + b_{23})^2 - 2C)c^2 + ((b_{11} + b_{23})^2 - 2C)^2)c^4 \\
&\quad + 2(C^2 - A^2)c^4 \\
&\quad + 2((b_{11} + b_{23})^2 - 2C)(C^2 - A^2)c^2 \\
&\quad + (C^2 - A^2)^2 \\
&= c^8 \\
&\quad + 2((b_{11} + b_{23})^2 - 2C)c^6 \\
&\quad + [(b_{11} + b_{23})^2 - 2C]^2 + 2(C^2 - A^2)c^4 \\
&\quad + 2((b_{11} + b_{23})^2 - 2C)(C^2 - A^2)c^2 \\
&\quad + (C^2 - A^2)^2
\end{aligned}$$

Now we can calculate the coefficients of the polynomial, for c^8 we have 1. For c^6 we have:

$$P = 2((b_{11} + b_{23})^2 - 2C) - (b_{12} + b_{24})^2$$

For c^4 we have

$$\begin{aligned} Q &= ((b_{11} + b_{23})^2 - 2C)^2 + 2(C^2 - A^2) \\ &\quad - 2(b_{12} + b_{24}) [(b_{11} + b_{23})B - (A + C)(b_{12} + b_{24})] \\ &\quad - ((b_{11} + b_{23})(b_{12} + b_{24}) - B)^2 \end{aligned}$$

For c^2 we have

$$\begin{aligned} R &= 2(C^2 - A^2)((b_{11} + b_{23})^2 - 2C) \\ &\quad - ((A + C)(b_{12} + b_{24}) - (b_{11} + b_{23})B)^2 \\ &\quad - 2B(A - C)(B - (b_{11} + b_{23})(b_{12} + b_{24})) \end{aligned}$$

and free term is

$$S = (C^2 - A^2)^2 - B^2(A - C)^2$$

Assume that $u = c^2$, then we obtain the equation:

$$u^4 + Pu^3 + Qu^2 + Ru + S = 0 \quad (56)$$

where

$$\begin{aligned} P &= 2((b_{11} + b_{23})^2 - 2C) - (b_{12} + b_{24})^2c^6, \\ Q &= ((b_{11} + b_{23})^2 - 2C)^2 - 2(b_{12} + b_{24})[(b_{11} + b_{23})B - (A + C)(b_{12} + b_{24})] \\ &\quad + 2(C^2 - A^2) - ((b_{11} + b_{23})(b_{12} + b_{24}) - B)^2, \\ R &= 2(C^2 - A^2)((b_{11} + b_{23})^2 - 2C) - 2B(A - C)[B - (b_{11} + b_{23})(b_{12} + b_{24})] \\ &\quad - [(A + C)(b_{12} + b_{24}) - (b_{11} + b_{23})B]^2, \\ S &= (C^2 - A^2)^2 - B^2(A - C)^2. \end{aligned}$$

Thus the constant c satisfies the equation (19). We solve equation (19) and find c^2 , which satisfies (19). Then we calculate X . Since $X = \cos(c\gamma)$, we finally obtain (20).

QED ■

5.4 Appendix 4

No we consider some applications of the general result of Theorem 1 to some special cases of our model. Consider the following system

$$n'(t) = (0.5F + \Phi)n(t - \gamma)\mathbf{D}(n(t - \gamma)) - 0.5d\frac{(n(t) - n_1(t))^2}{n(t)} - \Psi n(t), \quad (57)$$

$$n'_1(t) = \left[0.5F\frac{n_1(t - \gamma)}{n(t - \gamma)} + \Phi \right] \mathbf{D}(n(t - \gamma))n_1(t - \gamma) - \Psi n_1(t). \quad (58)$$

Then for $\gamma = 0$ we have

$$\begin{aligned} f_1(n, n_\gamma, n_1, n_{1\gamma}) &= (0.5F + \Phi)n_\gamma\mathbf{D}(n_\gamma) - 0.5d\frac{(n - n_1)^2}{n} - \Psi n, \\ f_2(n, n_\gamma, n_1, n_{1\gamma}) &= \left[0.5F\frac{n_{1\gamma}}{n_\gamma} + \Phi \right] \mathbf{D}(n_\gamma)n_{1\gamma} - \Psi n_1. \end{aligned}$$

Consider the case $\mathbf{D}(n^*) = e^{-\nu n^*}$ (where $\nu = -\ln(u)/2$, see (31)). Then

$$n^* = -\frac{1}{\nu} \log \mathbf{D}(n^*) = -\frac{1}{\nu} \log \left(\frac{(0.5F + \Phi)d \pm \sqrt{\Delta}}{F^2} \right).$$

and

$$b_{11} = \frac{\partial f_1}{\partial n} = -0.5d\frac{n^{*2} - n_1^{*2}}{n^{*2}} - \Psi, \quad b_{12} = \frac{\partial f_1}{\partial n_\gamma} = (0.5F + \Phi)(1 - \nu n^*)e^{-\nu n^*},$$

$$\begin{aligned}
b_{13} &= \frac{\partial f_1}{\partial n_1} = d \left(1 - \frac{n_1^*}{n^*} \right), \quad b_{14} = \frac{\partial f_1}{\partial n_{1\gamma}} = 0, \\
b_{21} &= \frac{\partial f_2}{\partial n} = 0, \quad b_{22} = \frac{\partial f_1}{\partial n_\gamma} = - \left[0.5F \frac{n_1^{*2}}{n^{*2}} + 0.5F\nu \frac{n_1^{*2}}{n^*} + \nu\Phi n_1^* \right] e^{-\nu n^*}, \\
b_{23} &= \frac{\partial f_2}{\partial n_1} = -\Psi, \quad b_{24} = \frac{\partial f_2}{\partial n_{1\gamma}} = \left[F \frac{n_1^*}{n^*} + \Phi \right] e^{-\nu n^*}.
\end{aligned}$$